Doctoral Dissertation (Censored)

博士論文 (要約)

Analyses of histone modification reprogramming and establishment of in vivo epigenome editing in medaka embryos

（ メダカ受精卵におけるヒストン修飾のリプログラミング動態解析と in vivo エピゲノム編集技術の確立 ）

A Dissertation Submitted for the Degree of Doctor of Philosophy

December 2020

令和２年１２月博士　(理学)　申請

Department of Biological Sciences, Graduate School of Science, The University of Tokyo

東京大学大学院 理学系研究科 生物科学専攻

Hiroto Fukushima

福嶋　悠人

Contents

Abbreviation

- ZGA : zygotic genome activation
- MZT: maternal zygotic transition
- ChIP: chromatin immunoprecipitation
- olKdm6ba: *Oryzias latipes*'s Kdm6ba
- RPKM: reads per kilobase per million mapped reads
- RPKMspike: spike-in normalized RPKM
- RPKMconv: conventional RPKM
- PRC: Polycomb repressive complex
- GO: gene ontology
- MNase: Micrococcal Nuclease
- TAD: topologically associating domain
- IMD: intermediately methylated domain
- HMM: hidden Markov model
- PRE: Polycomb response element
- HAT: histone acetyltransferase
- hsp300core: core domain (HAT domain) of *Homo sapiens*'s p300
- olEzh2: *Oryzias latipes*'s Ezh2
- sgRNA: single guide RNA
- olEzh2(ΔSET): SET domain deletion mutant of olEzh2

Abstract

In the last century, DNA sequence alone was regarded as the molecular entity of phenotypic inheritance. However, this view has been challenged by the findings of DNA sequence-independent inheritance in many species. Now, it is widely accepted that parental exposure to environmental stimuli, such as nutrient stress, physical stress, and chemical exposure, can affect traits in offspring, probably via inheritance of epigenetic modifications such as DNA methylation and histone modification from parental germ cells to offspring. However, compared to DNA methylation, it is not yet well characterized whether histone modifications can be inherited intergenerationally. This is due to the limited number of species in which their dynamics of histone-modification resetting after fertilization has been well studied, and also due to the lack of technology with which to assess the causality between epigenetic changes in germ cells and embryos. In this doctoral thesis, I took advantages of Japanese killifish, medaka (*Oryzias latipes*), and sought to solve these problems. In Chapter 1, to reveal epigenetic reprograming of histone modifications in medaka early development, I analyzed histone modification patterns after fertilization, genome-widely and quantitatively. As a result, the extensive erasure of histone modifications is further supported as conserved reprogramming mode among non-mammalian vertebrates. Furthermore, my study found retention of some modification during reprogramming and identified genetic and epigenetic characters, suggesting mechanisms and biological roles of pre-marking of those modifications, and possibility of intergenerational inheritance of such modifications. In Chapter 2, toward the future direct test of the inheritance of histone modifications, I established a technology of site-specific and *in vivo* histone modifications, or *in vivo* epigenome editing, in medaka embryo. My study will further help to understand the dynamics of epigenetic reprogramming among many species and to explore the possibility of intergenerational inheritance of histone modification in non-mammalian vertebrates.

General Introduction

We unconsciously recognize that our phenotypes are very similar to that of our parents. In the last century, this phenomenon was explained solely by the inheritance of DNA sequence based on the notion that DNA sequence (genetic information) alone is inherited across generations[1,2]. This notion was supported for a long time by the modern synthesis which was established in the mid-twentieth century by the combination of Darwin's evolutional theory and genetics[1,2]. Indeed, all cells in our body contain the same information of DNA sequence in spite of their very different and diverse identities, which was supported by John Gurdon's famous somatic reprogramming experiments[3]. However, this Gurdon's experiment also indicates that DNA sequence alone is not sufficient to establish our whole phenotype.

From the late twentieth century, the idea of epigenetics was gradually established[2], and epigenetic modification to chromatin has become one of the most important subjects in modern biology. Epigenetic modification includes methylation to cytosine in DNA strand, several chemical modifications to histone proteins such as methylation and acetylation (Figure 1). These epigenetic modifications positively and negatively associate with transcriptional states[4,5] (Figure 1). In general, the pattern of these modifications can be epigenetically transmitted from a mother cell to daughter cells by self-maintenance mechanisms (e.g. maintenance methylation mechanism of DNA methylation[6] and self-propagation of H3K9me3 and H3K27me3[7]). Epigenetic modification is thus considered as a second layer of information associated with DNA, controlling the establishment and maintenance of cellular identities for the entire life of multicellular organisms by such stable inheritance across cell generations and transcriptional function, leading to proper organization of our whole body[8,9] (Figure 1). Actually, epigenetic modification has been implicated in the maintenance of pluripotency, lineage-specific cell differentiation and pathological transformation including cancer and neurological disease[5,8,10].

Recently, many cases of DNA sequence-independent inheritance across

generations were reported, challenging the previous view of DNA-alone inheritance, and epigenetic modification and its inheritance, or epigenetic inheritance, have drawn attention[1,11–13]. For example, we now know that parental exposure to environmental stimuli, such as nutrient stress, physical stress, and chemical exposure can affect traits in offspring[1,11–13], reminding us of the Lamarck's idea of inheritance of acquired tratis[14]. Given that such exposure easily triggers alterations of parental phenotypes associated with epigenetic modifications without mutations in DNA sequence, such inheritance appears to be mediated by epigenetic inheritance, not by DNA sequence inheritance. Importantly, DNA sequence-independent inheritance of such phenotypes was observed not only between parents and children (termed "intergenerationally"), but also across multiple generations, i.e. from parent to children, grandchildren, and so on (termed "transgenerationally")[1,11,12].

Inter- and trans-generational inheritance of DNA methylation has been intensively investigated for a long time, and there are many previous studies in mammals, reporting the association between altered phenotypes in offspring induced by parental exposures to environmental stimuli and changes in DNA methylation pattern[15–18]. For example, some mother rats naturally show frequent nurturing such as grooming, while others do not, and the nurturing frequency in rats is well correlated with that of their mothers[19]. Interestingly, this maternal care phenotype is associated with DNA methylation in the glucocorticoid receptor gene and its expression level, and importantly, the phenotype and DNA methylation level can be reversed by cross-fostering[19]. Furthermore, inheritance of DNA methylation throughout many generations is frequently demonstrated in plants, such as naturally occurred stable epimutant lines in tomato[20] and *Linaria vulgaris*[21], and also stable inheritance of artificially altered DNA methylation patterns in *Arabidopsis thaliana*[11].

Histone modification is another possible candidate mediating DNA sequence-independent inheritance[1,11,12]. One of the most well-studied examples in animals is transgenerational inheritance in *C. elegans*[12]. Furthermore, in vertebrates, it was previously

shown that disruption of histone modifications in sperm triggered impaired transcription and caused abnormal phenotypes in offspring in *Xenopus*[22] and mouse[23,24]. However, intergenerational epigenetic inheritance of histone modification is not fully understood in animals, largely due to its relatively recent findings, compared to DNA methylation. There remain many unanswered questions regarding the epigenetic inheritance of histone modification. First, experimental evidence showing the direct causality between epigenetic and phenotypic changes in offspring is still poor. *C. elegans* is exceptional in that the causality has been well tested by taking advantages of various rich mutants[12]. However, mutations that globally disrupt epigenetic landscape tend to be lethal in many other species[25], making it difficult to broadly examine the causality. Second, it is known that histone modifications are extensively reprogrammed during gametogenesis and early embryogenesis[26] (Figure 2). This complicates the study of epigenetic inheritance, raising a question of whether an alteration in epigenetic landscape in parental germ cells induced by external exposure can escape reprogramming and how escaped modifications affect offspring phenotypes inter- or trans-generationally. Indeed, the dynamics of histone modification reprogramming has not been well documented yet in many species, especially in non-mammalian species, limiting our understanding of conservation or diversity of histone modification reprogramming.

In my doctoral thesis, I sought to solve these problems and extend our understanding of intergenerational epigenetic inheritance in non-mammalian vertebrates. Here, I use Japanese killifish, medaka (*Oryzias latipes*) with various experimental advantages such as availability of genetic and epigenetic manipulation[27], high quality genome (N50: ~2.5 Mbp, gaps: ~500)[28], relatively small genome size among vertebrates (~800Mb)[28], rich epigenetic and transcriptomic data published so far[28–30], rapid life cycle (~three month / one generation)[31], previous reports of intergenerational effects of parental exposure to endocrine disrupters[32,33], and so on. In Chapter 1, to find any genomic regions where histone modifications escape reprogramming during early normal development, I

quantitatively and genome-widely revealed how histone modifications are reprogrammed after fertilization in medaka. However, I thought that even if there are any genomic regions where certain histone modifications escape reprogramming, the following two possibilities remain. One is that those remaining histone modifications are a consequence of direct transmission, that is, in a DNA sequence-independent manner, from germ cells to embryos. The other is that they are a result of *de novo* accumulation of such modifications after fertilization in a sequence-dependent manner, recreation of normal pattern of histone modifications encoded by the genome. Thus, to distinguish the two possibilities, a novel approach that can ectopically induce histone modifications is required for a direct test on inheritance of histone modifications across generations. For this purpose, in Chapter 2, I newly established a method for site-specific manipulation of histone modification *in vivo*. I hope that my study will further help to understand the dynamics of epigenetic reprogramming among many species and to explore the possibility of intergenerational inheritance of histone modification in non-mammalian vertebrates.

Chapter 1: Analyses of histone modification reprogramming in medaka embryos

本章については、5 年以内に雑誌等で刊行予定のため、非公開

Chapter 2: Establishment of in vivo epigenome editing in medaka embryos

Introduction

In Chapter 1, retention of H3K27ac and H3K27me3 was observed in early embryos before reprogramming and thus those modifications are candidates that can be intergenerationally inherited in medaka. It is thought that epigenetic modifications, when inherited, affect expression of nearby genes in offspring. To test the causality of epigenetic alteration and phenotypic inheritance, a technology manipulating epigenetic modifications is required. For this purpose, in *C. elegans*, mutant lacking writers of histone modifications was used[12]. However, such mutation globally disrupts transcription, causing severe phenotypes and/or embryonic lethality, which made it difficult to examine the heritability of histone modifications in vertebrates[25]. Indeed, such global epigenetic alteration might trigger misdistribution of other epigenetic modifications, because epigenetic landscape is a result of interaction of many modifications. In this case, it is more difficult to distinguish primary and secondary causes for phenotypic inheritance. Therefore, a technology manipulating a modification directly and site-specifically to the genome is required for the study of epigenetic gene regulation and inheritance.

The establishment of targeted direct manipulation of epigenetic modification is also important in terms of cell biology or developmental biology. Recent studies using next generation sequencing techniques have revealed genome-wide associations between epigenetic modifications and transcriptional states[4]. However, a lack of technologies for targeted manipulation of histone modifications at individual genomic loci has hindered the progress toward demonstrating a causal relationship between specific modifications and their effect on transcriptional regulation. For example, H3K27me3 is a repressive histone modification, and thought to be important for long-term transcriptional repression[9]. In the proposed model of long-term repression by H3K27me3, Polycomb repressive complex 2 (PRC2) is first recruited to its target sites, and the H3K27 methyltransferase Ezh2 catalyzes

H3K27me3. Subsequently, PRC1 binds to H3K27me3 and silences the chromatin[34,35]. On the other hand, histone acetyltransferase p300 induces H3K27ac, which is associated with open chromatin and transcription factor binding to DNA[36]. Indeed, previous genome-wide analysis are generally consistent with these models; H3K27ac is mainly associated with active enhancers, promoters and transcription start sites, while H3K27me3 correlates with repressed or poised promoters and enhancers[4]. The proposed models were based on results from *in vitro* biochemical studies, *in vivo* overexpression, knock-out and knock-down experiments of epigenetic modifying enzymes. However, many of these studies could not exclude the possibility of indirect secondary effects, because such manipulations alter the epigenome in a genome-wide way. Furthermore, recent studies suggested that H3K27me3 deposition could be a consequence of transcriptional repression[37,38]; PRC1 recruitment can subsequently cause PRC2 protein binding in certain genomic regions[39,40], in particular, at previously active promoters, which results in the accumulation of H3K27me3[41]. Thus, even now, it is unclear whether H3K27me3 accumulation alone is sufficient to repress transcription of nearby genes. As discussed above, H3K27me3 has also been proposed to function as epigenetic memory, which enables the long-term maintenance of a cell-type specific transcriptional state in normal development[8]. However, it is unknown whether histone modifications themselves can be inherited across cell generations, and function as epigenetic memory for a long time. Therefore, direct manipulation of H3K27me3 at individual genomic loci is required to fully understand the mechanism of H3K27me3-associated repression, in addition for the study of direct heritability of histone modification.

One possible approach for site-specific epigenetic modification is to manipulate target DNA sequences. Polycomb response elements (PREs; a combination of transcription factor motifs) were discovered in *Drosophila*[35,38,42,43] and *Arabidopsis thaliana*[44] and are well-studied as consensus recruiter sequences that bind PRC2 through interaction with other DNA binding factors. Thus, in such organisms, the deletion or addition of the PRE results in the

site-specific reduction or accumulation of H3K27me3[45,46]. However, a consensus recruiter sequence like PREs has not been discovered in other organisms such as vertebrates[42]. In addition, *in vivo* manipulation of DNA sequence could affect binding of other factors. It also requires the establishment of transgenic animals, which is still a difficult and time-consuming process. Thus, an alternative technique for *in vivo* targeted epigenome editing of H3K27me3 has been needed.

CRISPR-based dCas9 epigenome editing was recently developed as an alternative method for targeted epigenetic manipulation[34]. dCas9 is the nuclease-null deactivated Cas9 which has mutations in the RuvC and HNH domains[47]. Like the CRISPR-Cas9 system, a single-guide RNA (sgRNA) guides modifying enzymes or domains fused to dCas9 to the targeted genomic locus, which alters the epigenetic state at the site. In principle, this method could be applied to any organism, unlike the deletion of the consensus recruiter sequence. However, the number of editable modifications and reports using the dCas9 system *in vivo* or *in vivo* epigenome editing are still limited[48–56].

In this chapter, I aimed to develop a robust *in vivo* epigenome manipulation method using medaka (Japanese killifish, *Oryzias latipes*) embryos. I generated a new construct, dCas9-olEzh2 (*Oryzias latipes* Ezh2 fused to dCas9), for manipulating H3K27me3, and demonstrated that dCas9-olEzh2 accumulated H3K27me3 at specific targeted loci and induced gene repression[27]. These *in vivo* epigenome editing will help in the study of epigenetic regulation of gene expression and heritability of epigenetic modifications at particular genomic loci.

Results

Injection of dCas9-hsp300core mRNA in medaka embryo can activate target gene expression *in vivo*

To test whether I can apply a technology of dCas9 epigenome editing in medaka embryos, I used the dCas9-hsp300core construct which was previously shown *in vitro* to activate gene expression through site-specific H3K27ac manipulation[48]. In this construct, a Bromo domain, which recognizes acetylated lysine residues on histone tails, and histone acetyltransferase (HAT) domain of human p300 (hsp300core) were fused to dCas9 with a FLAG tag at the N-terminus (Figure 28A). The Bromo and HAT domains are highly conserved among human, mouse, zebrafish and medaka (Figure 27), suggesting that this construct can also induce site-specific H3K27ac in medaka. In the previous study, several genes including *Myod* were modified by dCas9-hsp300core transfection in cultured human cells[48]. Thus, I also chose medaka *Myod1* as a target gene and injected dCas9 or dCas9-hsp300core mRNA along with three sgRNAs targeting the medaka *Myod1* promoter (Figure 28B, 28C). I used a set of sgRNAs targeting a single promoter region because previous studies showed that multiple sgRNAs at each target promoter increased the efficiency of epigenome editing[47,57,58]. To detect dCas9-hsp300core recruitment and H3K27ac induction at the target loci, I performed ChIP-qPCR at the late blastula stage (stage 11), when histone modifications have already been accumulated after epigenetic reprogramming[30,59] (Figure 28B). ChIP-qPCR using anti-FLAG antibody showed that dCas9 and dCas9-hsp300core were efficiently and specifically recruited to the target sites (Figure 28D), but ChIP-qPCR using anti-H3K27ac antibody revealed that there was no significant accumulation of H3K27ac in embryos injected with dCas9-hsp300core (Figure 28E). The positive and negative control regions for ChIP experiments are described in (Figure 29). I then tested whether gene expression was affected, using RT-qPCR. For this expression analysis, the pre-early gastrula (stage 12) embryos were

used, which follows the zygotic genome activation (ZGA) at the late blastula stage (stage 11)[60]. Importantly, RT-qPCR of medaka *Myod1* at the pre-early gastrula stage (stage 12) showed upregulation in samples from dCas9-hsp300core-injected embryos (Figure 28F). These results suggest that the dCas9-hsp300core protein can site-specifically activate gene expression, but its ability to induce H3K27ac is low in medaka. It is possible that even though the HAT activity of dCas9-hsp300core is low in medaka, the level of H3K27ac induced by dCas9-hsp300core is sufficient to effectively activate gene expression. Alternatively, since p300 can function not only as an acetyltransferase, but also as a scaffold for recruiting other activators[61], the p300 core domain may activate gene expression through an additional, unknown mechanism. In addition, acetylation on other histone residue H3K122 (H3K122ac) is also catalyzed by p300 and H3K122ac is sufficient to directly stimulate transcription[62]. Therefore, it is also possible that not H3K27ac but H3K122ac was deposited by dCas9-hsp300core and triggered transcription of target gene in my system.

dCas9-olEzh2 injection in medaka results in site-specific accumulation of H3K27me3 *in vivo*

In order to make a new construct for *in vivo* H3K27me3 manipulation by dCas9 epigenome editing, I first cloned the *Oryzias latipes* H3K27 methyltransferase Ezh2 (olEzh2) sequence and compared it with human, mouse, and zebrafish Ezh2 sequences. The alignment revealed that Ezh2 is highly conserved (98%) among the vertebrate species, especially the CXC domain and the SET domain (100%), which are required for H3K27 methyltransferase activity (Figure 30).

To test the ability of olEzh2 to induce H3K27me3 site-specifically *in vivo*, full-length olEzh2 was fused to dCas9 with a FLAG tag at the N-terminus (Figure 31A). To select target genome regions for H3K27me3 manipulation, I investigated previously published ChIP-seq data from medaka blastula embryos[30]. I selected promoter regions of 7 genes, *Arhgap35,*

Pfkfb4a, *Nanos3*, *Dcx*, *Tbx16, Slc41a2a* and *Kita* as targets, because they showed low H3K27me3 enrichment at the blastula stage (Figure 31C, 31G, 31K, 31N, 33A, 33D, 34F). These target promoters do not show any particular characteristics in terms of CpG contents compared to others. sgRNAs were designed to target DNase I hyper sensitive sites using DNase I-seq data from medaka blastula[63], because previous genome-wide Cas9 binding studies showed that chromatin inaccessibility prevents sgRNA / Cas9 complex binding[64,65]. I used a set of sgRNAs targeting a single promoter region because previous studies showed that multiple sgRNAs at each target promoter increased the efficiency of epigenome editing[47,57,58].

I injected dCas9 or dCas9-olEzh2 mRNA along with three or four sgRNAs into medaka the one-cell-stage (stage 2) embryos, and to examine the recruitment of dCas9 or dCas9-olEzh2 and accumulation of H3K27me3 at the target regions, I performed ChIP-qPCR at the late blastula (stage 11), when histone modifications have already been accumulated after epigenetic reprogramming[30,59] (Figure 31B). For each target promoter, several primer pairs that overlap with sgRNAs were designed for ChIP-qPCR. The positive and negative controls for ChIP experiments are described in Figure 29. The results of ChIP-qPCR using anti-FLAG antibody confirmed that dCas9-olEzh2 was recruited specifically to the target sites (Figure 31D, 31H, 31L, 31O, 33B, 33E, 34G). Importantly, at *Arhgap35, Pfkfb4a, Nanos3*, *Dcx* and *Kita* loci, the level of H3K27me3 increased in dCas9-olEzh2 injected embryos, as compared to non-injected and dCas9 injected ones (Figure 31E, 31I, 31M, 31P, 33H), demonstrating that dCas9-olEzh2 is capable of inducing site-specific H3K27me3 *in vivo*. On the other hand, at *Tbx16* and *Slc41a2a* loci, there was no significant induction of H3K27me3 (Figure 33C, 33F), even though dCas9-olEzh2 was recruited to the target site (Figure 33B, 33E). I hypothesized that some factors were preventing the accumulation of H3K27me3 at these two loci. Analysis of published whole-genome bisulfite sequencing data from medaka blastula embryos[29] revealed that *Arhgap35*, *Pfkfb4a, Nanos3*, *Dcx* and *Kita* promoters are

hypomethylated (Figure 31C, 31G, 31K, 31N, 34F), whereas *Tbx16* and *Slc41a2a* promoters are highly methylated (Figure 33A, 33D). Antagonism between DNA methylation and H3K27 methylation was previously reported in mouse embryonic stem cells[66] and neural stem cells[67] and also in medaka blastula embryos[30], and therefore pre-existing DNA methylation might have inhibited the induction of H3K27me3 by dCas9-olEzh2 at *Tbx16* and *Slc41a2a* promoters.

Since the antagonism between H3K27me3 and H3K27ac has also been reported[68], I further checked whether the level of H3K27ac was affected by the dCas9-olEzh2-induced H3K27me3 accumulation. However, ChIP-qPCR using anti-H3K27ac antibody at the *Arhgap35* promoter in the sgArhgap35 / dCas9-olEzh2 injected embryos showed no significant differences (Figure 32), suggesting that the level of H3K27me3 induced by dCas9-olEzh2 was not sufficient for a detectable level of H3K27ac reduction.

Induced H3K27me3 strengthens site-specific gene repression

Next, I examined whether the induction of H3K27me3 by dCas9-olEzh2 has the function to repress the expression of targeted genes, as H3K27me3 induced by Ezh2 is known as a repressive histone modification[35,43]. To investigate the repression capacity of dCas9-olEzh2, I chose the zygotically transcribed genes, *Arhgap35*, *Pfkfb4a* and *Kita* among the five targets that showed H3K27me3 induction. I injected dCas9-olEzh2 mRNA along with sgRNAs targeting the *Arhgap35,* the *Pfkfb4a* or the *Kita* promoter, and performed RT-qPCR at the pre-early gastrula stage (stage 12) (Figure 31B), which follows the zygotic genome activation (ZGA) at the late blastula stage (stage 11) [60]. As a result, both dCas9 and dCas9-olEzh2 injected embryos showed downregulation of *Arhgap35, Pfkfb4a* or *Kita* compared to non-injected ones (Figure 31F, 31J, 34I), and this agrees with a previous report indicating that dCas9 itself can interfere with transcriptional elongation, RNA polymerase binding, or transcription factor binding[47]. Importantly, the expression of *Arhgap35* and *Kita* in dCas9-

olEzh2-injected embryos was significantly lower than that in dCas9-injected ones (Figure 31F, 34I), suggesting that H3K27me3 have strengthened the repression. On the other hand, the expression level of *Pfkfb4a* did not show significant difference between dCas9 and dCas9-olEzh2 injected embryos (Figure 31J). Thus, the effect of H3K27me3 accumulation to gene expression may be different between genes, or the levels of H3K27me3 accumulation at *Pfkfb4a* promoter was too low (Figure 31I).

To validate that the H3K27me3 deposition is causative of transcriptional repression of target genes, I generated a SET domain-deleted mutant dCas9-olEzh2(ΔSET) (Figure 31A). First, I confirmed that this construct had no ability to induce H3K27me3 at target sites (Figure 34A, 34B, 34G, 34H). Then, I found that the expressions of the two target genes, *Arhgap35* and *Kita*, were significantly lower in dCas9-olEzh2 injected embryos than in dCas9 or dCas9-olEzh2(ΔSET)-injected ones (Figure 34C, 34I). To further test the possibility that transcriptional interference by dCas9 complex caused the H3K27me3 deposition[37,38], I increased the molecular concentration of dCas9-olEzh2(ΔSET) up to 550 nM, and inhibited the gene expression at the same level as dCas9-olEzh2 injection. (Note that all other experiment in this paper used 350 nM concentration.) Under this condition, dCas9-olEzh2(ΔSET) (550 nM)-injected embryos showed strong reduction in transcription of the targeted gene (Figure 34D). However, neither dCas9-olEzh2(ΔSET) (350 nM)-injected embryos nor dCas9-olEzh2(ΔSET) (550 nM)-injected embryos showed the accumulation of H3K27me3 at the target region (Figure 34E). Thus, I concluded that the deposition of H3K27me3 was caused by the enzymatic activity of dCas9-olEzh2, but not by transcriptional interference.

H3K27me3 epigenome editing by dCas9-olEzh2 is highly site-specific

Finally, to globally confirm the specificity of H3K27me3 epigenome editing by dCas9-olEzh2, I performed ChIP-seq of dCas9-olEzh2 mRNA / sgArhgap35 sgRNA-injected or dCas9-

olEzh2(ΔSET) mRNA / sgArhgap35 sgRNA-injected late blastula (stage 11) embryos using anti-FLAG antibody and anti-H3K27me3 antibody. First, I confirmed that two biological replicates showed consistent distribution of dCas9 binding and H3K27me3 (Figure 35A-D). Thus, in the following analyses, I pooled two replicates. Next, I confirmed the specificity of dCas9-olEzh2(ΔSET) and dCas9-olEzh2 recruitment to the target site (Figure 36A, 36B). Finally, I observed that H3K27me3 was only induced at the sgRNA target region in dCas9-olEzh2-injected embryos, while there was no deposition of H3K27me3 in dCas9-olEzh2(ΔSET)-injected embryos (Figure 37A, 37B). Among all H3K27me3 peaks in dCas9-olEzh2(ΔSET) and dCas9-olEzh2-injected embryos, only H3K27me3 enrichment of the sgRNA target region was significantly changed (Figure 37C, 37D). These data demonstrate the high specificity of H3K27me3 epigenome editing by dCas9-olEzh2.

Discussion

In this study, I generated dCas9-olEzh2 for manipulating H3K27me3, and demonstrated that co-injection of three or four sgRNAs and dCas9-olEzh2 mRNA into the one-cell-stage medaka embryos induced accumulation of H3K27me3 at specific targeted loci and significant reduction in gene expression (Figure 38).

DNA methylation and he ability of dCas9-olEzh2 to induce H3K27me3

So far I tested, the ability of dCas9-olEzh2 to induce H3K27me3 was limited to hypomethylated regions (Figure 38). A previous study using dCas9-PRDM9 (H3K4 methyltransferase PRDM9 fused to dCas9) suggested that dCas9 itself was not able to bind to highly methylated genomic regions[50]. However, my dCas9-olEzh2 successfully bound to methylated target sites. Importantly, I chose the target sites that are DNase I-hypersensitive, as previous genome-wide Cas9 binding studies showed that the binding of sgRNA / Cas9 complex depends on chromatin accessibility[64,65]. Taken together, my results suggest that dCas9-olEzh2 is able to bind to methylated sites if the chromatin is accessible, but the induction of H3K27me3 is prohibited by other inhibitory role of DNA methylation against Ezh2 (Figure 38). However, I can not exclude the possibility that the binding efficiency of sgRNA affected H3K27me3 accumulation to methylated promoters.

H3K27me3 and gene repression

Interestingly, the most recent study using human cell lines and mouse Ezh2 fused to dCas9 N-terminus (Ezh2-dCas9) reported that H3K27me3 induction at *HER2* promoter did not correlate with transcriptional repression[69]. Also in this study, the two targets (*Arhgap35* and *Kita*) out of the three showed significant downregulation of gene expression, whereas the one (*Pfkfb4a*) of three targets did not. These results suggest that the effect of H3K27me3 on

transcription differs among gene loci. Furthermore, the downregulation of target genes (*Arhgap35* and *Kita*), though statistically significant, appeared modest. This suggests that induced H3K27me3 deposition was not sufficient for strong repression under my experimental conditions or other factors, such as H3K9me or repressor binding, are further required for complete suppression of gene transcription of these genes. In addition, since the deposition of H3K27me3 did not induce the detectable change of H3K27ac level (Figure 32), sufficient repression might require de-acetylation.

Further applicability of H3K27me3 epigenome editing

Thus far, dCas9-based epigenome editing was reported to site-specifically manipulate H3K27me3[69], H3K27ac[48], H3K9me3[49], H3K4me3[50], H3K79me2[50], and DNA methylation[51–53] under *in vitro* conditions. *In vivo* dCas9-based epigenome editing applications has been used for site-specific deubiquitylation by injection in nuclear transferred *Xenopus* oocyte[55], targeted manipulation of DNA methylation in mouse oocyte by injection[56], and in mouse brain by *in vivo* electrophoresis[52,53]. The present study is the first to site-specifically manipulate H3K27me3 *in vivo*, and extends the applicability of the *in vivo* dCas9-based epigenome editing. Dysregulation of H3K27me3 has been implicated in diseases such as cancer[70,71]. Given that Ezh2 is highly conserved among vertebrates including human, my dCas9-olEzh2 system can be a model for *in vivo* disease treatment in the future.

Materials and Methods

medaka strain and developmental stages

Medaka d-rR strain was used for all experiments in this study. Medaka fish were maintained and raised according to standard protocols. Developmental stages were determined based on previously published guidelines[72].

cloning and alignment

Total RNA from two days-post-fertilization medaka embryos was reverse transcribed to a cDNA mix, using SuperScript III First-Strand Synthesis SuperMix (Invitrogen, 18080400). Medaka Ezh2 (olEzh2) was amplified from this cDNA mix using cloning primers (described in Table S1), and PCR products were cloned into the pCR2.1-TOPO vector (pCR2.1-olEzh2). Human, mouse and zebrafish canonical Ezh2 coding DNA sequence (CDS) were obtained from Ensembl (human : ENSP00000419711, mouse : ENSMUSP00000080419, zebrafish : ENSDARP00000023693). These sequences were aligned using T-Coffee[73], and the colored alignment figure was made using the Sequence Manipulation Suite[74].

sgRNA design

sgRNAs were designed using CCtop CRISPR / Cas9 target online predictor[75] with default parameters except the target site length. I set the target site length to 18. The sgRNA target sequences and locations are described in Table S1.

plasmid construct

Cas9 sequence in pMLM3613 (Addgene, #42251) was modified (D10A and H840A) by PrimeSTAR® Mutagenesis Basal Kit (Takara, R046A) using mut.1 and mut.2 primers. This dCas9 sequence was amplified by primers containing FLAG and NLS sequences, then it was

assembled with XbaI-linearized pCS2+ vector (pCS2+-dCas9) using NEBuilder HiFi DNA Assembly Master Mix (NEB, E2621). From pCR2.1-olEzh2, olEzh2 sequence was amplified and assembled with XhoI-linearized pCS2+-dCas9 vector (pCS2+-dCas9-olEzh2) using NEBuilder. To make pCS2+-dCas9-olEzh2(ΔSET) plasmids, I modified olEzh2 sequence in pCS2+-dCas9-olEzh2 by PrimeSTAR® Mutagenesis Basal Kit (Takara, R046A) using mut-olEzh2-ΔSET primers. I constructed the sgRNA vectors from pDR274 (Addgene, #42250) based on the method described in previous paper[76]. All primers used for construction are described in Table S2.

in vitro transcription

dCas9, dCas9-olEzh2 and dCas9-olEzh2(ΔSET) mRNA were generated using PCR products from pCS2+-dCas9, pCS2+-dCas9-olEzh2, pCS2+-dCas9-olEzh2(ΔSET) as templates, respectively, which contain T7 promoters. mRNA was synthesized using HiScribe T7 ARCA mRNA kit (NEB, E2060S). sgRNAs were synthesized using PCR products of sgRNA vectors as templates and HiScribe T7 Quick High Yield RNA Synthesis Kit (NEB, E2050S). RNeasy mini kit (QIAGEN, 74104) was used to purity RNA. Primers for PCR amplification of the *in vitro* transcription template are described in Table S2.

RNA Injection and ChIP-qPCR

For dCas9-olEzh2 injection, either dCas9-olEzh2 mRNA, dCas9-olEzh2(ΔSET) or dCas9 mRNA along with three or four sgRNAs (120 ng / μL each) were injected into the one-cell stage (stage 2) embryos. To roughly normalize the number of molecules per injection (350 nM), dCas9-olEzh2, dCas9-olEzh2(ΔSET) and dCas9 mRNA were injected at concentration of 750 ng / μL, 710 ng / μL or 500 ng / μL. For higher concentration injection of dCas9-olEzh2(ΔSET), dCas9-olEzh2(ΔSET) mRNA (1100 ng / μL, 550 nM) and sgRNAs (180 ng / μL) were injected. After 8 hours of incubation, the late blastula (stage 11) embryos were

transferred into PBS containing 20 mM sodium butyrate, 1 mM PMSF, and 1 x cOmplete EDTA-free Protease Inhibitor Cocktail (Roche, 11873580001), and cells were gently dissociated using homogenizer (BMBio, C-3452-2) or gentle pipetting (about 150 embryos for dCas9-olEzh2 injection ChIP, and about 50 embryos for dCas9-olEzh2(ΔSET) injection ChIP). Subsequently, cells were cross-linked by adding formaldehyde (1 % volume per volume final) for 8 minutes at room temperature then quenched by adding glycine (200 mM final). After washing with PBS containing 20 mM sodium butyrate, 1 mM PMSF, and 1 x Protease Inhibitor Cocktail, cross-linked cells were stored in -80°C as dry pellet. For dCas9-olEzh2 injection ChIP, all subsequent procedures were performed as previously described[30]. For dCas9-olEzh2(ΔSET) injection ChIP, cross-linked cells were sonicated in a microTUBE AFA Fiber Snap-Cap 6x16mm (Covaris, 520045) using Covaris S220 with optimized parameters (Peak Power : 105, Duty Factor : 4.0, cycles per burst : 200, duration : 750 seconds), and all subsequent procedures were performed as previously described[30]. Anti-FLAG antibody (Sigma, F3165), anti-histone H3K27ac antibody (abcam, ab4729) and anti-histone H3K27me3 antibody (Millipore, 07-449 for sgArhgap35, sgTbx16, sgNanos3 and sgDcx, or Diagenode, c15410069 for sgArhgap35, sgKita, sgPfkfb4a and sgSlc41a2a) were used for each experiment. All primers for ChIP-qPCR are described in Table S3.

RT-qPCR

For sgArhgap35, sgKita and sgPfkfb4a RT-qPCR, either dCas9-olEzh2 mRNA (750 ng / μL), dCas9-olEzh2(ΔSET) (710 ng /μL) or dCas9 mRNA (500 ng / μL) was injected along with three or four sgRNAs (120 ng / μL each) into the one-cell stage (stage 2) embryos. For higher concentration injection of dCas9-olEzh2(ΔSET), dCas9-olEzh2(ΔSET) mRNA (1100 ng / μL, 550 nM) and sgRNAs (180 ng / μL) were injected. After 10 hours of incubation, the pre-early gastrula (stage 12) embryos (50 embryos) were homogenized and all subsequent steps were performed as previously described[30]. All primers for RT-qPCR are described in Table S4.

ChIP-seq library preparation and sequencing

I generated two biological replicates for ChIP-seq. ChIP was performed following the protocol described above. After ChIP, ChIP-seq libraries were prepared using KAPA Hyper Prep Kit (KAPA Biosystems, KK8504). All ChIP-seq libraries were sequenced using Illumina HiSeq1500 system.

ChIP-seq data processing

First, low quality reads and adapter-derived sequences were trimmed by Trimmomatic[77]. Second, trimmed-reads were aligned to medaka genome (MEDAKA1) using BWA[78]. Third, I removed alignments with mapping quality smaller than 20. Finally, MACS2[79] was used to call peaks (q-value < 0.01) and to generate signals per million reads tracks.

ChIP-seq analysis

To test the correlation of the two biological replicates, reads per kilobase per million mapped reads (RPKM) for each 5 kb bin was calculated, Pearson's correlation coefficient was calculated.

To check the specificity of dCas9-olEzh2 targeting, I plotted fold-enrichment of FLAG ChIP-seq signals by calculating the ratio between the ChIP sample signals and the local control lambda outputted by MACS2[79].

To investigate the fold change of H3K27me3 enrichment in peaks in dCas9-olEzh2 injected embryos and dCas9-olEzh2(ΔSET) embryos, I followed the procedure described in the previous study[49]. I pooled two replicates, called peaks using MACS2[79], merged H3K27me3 peaks of each condition using bedtools merge[80], calculated the read number overlapping the merged peaks in each replicates using bedtools intersect[80], and compared H3K27me3 enrichment and fold change using DESeq2[81].

Statistics

The experiments shown in Figure 31F, 34C, 34D and 34Ii had six biological replicates, ChIP-seq experiments had two biological replicates, and all other experiments in this study had three biological replicates. Student's t-test was used to compare two groups in Fig. 31F, and 31J. Tukey-Kramer test was used to compare groups in the ChIP-qPCR and RT-qPCR analyses of all other experiments. Data are expressed as mean ± s.d.

Conclusion

Intergenerational inheritance of histone modifications was widely recognized in recent years, yet it is currently unclear to what extent this phenomenon is essential for development and physiology of progeny in vertebrates. This is mainly due to the limited number of non-mammalian species whose reprogramming processes during early development are intensively examined, and also to the lack of the target-specific and direct manipulation technology *in vivo*.

In Chapter 1, to extend the understanding of reprogramming of histone modifications after fertilization in non-mammalian vertebrates, I performed genome-wide and quantitative analysis of histone modification reprogramming in medaka embryos. As a result, I found that all modifications are erased more or less after fertilization, but that H3K27ac, H3K27me3 and H3K9me3 largely or partially escape erasure (Figure 26A). This analysis further supports conservation of extensive erasure of histone modifications during reprogramming among non-mammalian vertebrates (Figure 26B). With further analysis using previous RNA-seq and ATAC-seq data, I discussed the function of H3K27ac pre-marking and the possibility of H3K27me3 transmission from parental germ cells (Figure 26A). Consistently, medaka sperm ChIP-seq also revealed the overlap of H3K27me3 accumulation in blastula and sperm (Figure 26A). My quantitative data of various histone modifications will make medaka a good non-mammalian platform with which to analyze conserved and diverse features of epigenetic reprogramming in the vertebrate lineage. However, to directly analyze transmission of histone modifications from germ cells to offspring, development of *in vivo* epigenome editing technology was definitely needed.

In Chapter 2, toward the establishment of technology of direct and target site-specific in vivo manipulation of histone modification, I sought to apply dCas9 system to medaka embryos. As a result, I succeeded in developing targeted induction of H3K27me3 in medaka embryos by mRNA injection and confirmed its targeting specificity (Figure 38).

Furthermore, the deposition of H3K27me3 in promoter resulted in downregulation of downstream gene, suggesting the causal relationship between H3K27me3 and gene repression (Figure 38). This success, however, is only a first step, as I further need to establish epigenome editing in germ cells in order to directly test the intergenerational epigenome inheritance.

Toward further understanding of intergenerational epigenetic and phenotypic inheritance, it will further be required to experimentally demonstrate whether histone modifications in parental germ cells are inherited to embryos and affect development of offspring in non-mammalian vertebrates (Figure 39). Since I found the possibility of intergenerational H3K27me3 transmission and also established *in vivo* H3K27me3 epigenome editing, medaka can be an ideal vertebrate model to address such unanswered questions. Further studies are awaited in future, for example establishment of transgenic lines for *in vivo* epigenome editing in sperm and oocytes, or direct injection of *in vivo* epigenome editing in oocyte.

In this doctoral thesis, I mainly focused on histone modifications and their inheritance. However, other epigenetic factors such as DNA methylation and small RNAs may serve for phenotypic inheritance. Previous studies showed that small RNAs in sperm contributed to the phenotypic changes of offspring induced by parental exposure to environmental stimuli in mice[82,83], and indeed small RNAs were found in medaka germ cells[84]. Remarkably, DNA methylation in zebrafish was found not to undergo reprogramming[85–89] unlike in mammals, and stable transmission of DNA methylation pattern across generations was experimentally demonstrated in medaka[90]. Thus, I speculate that not only histone modifications but also other epigenetic factors such as small RNAs and DNA methylation in parental germ cells contribute independently and/or synergistically to embryonic development.

Figures and Legends

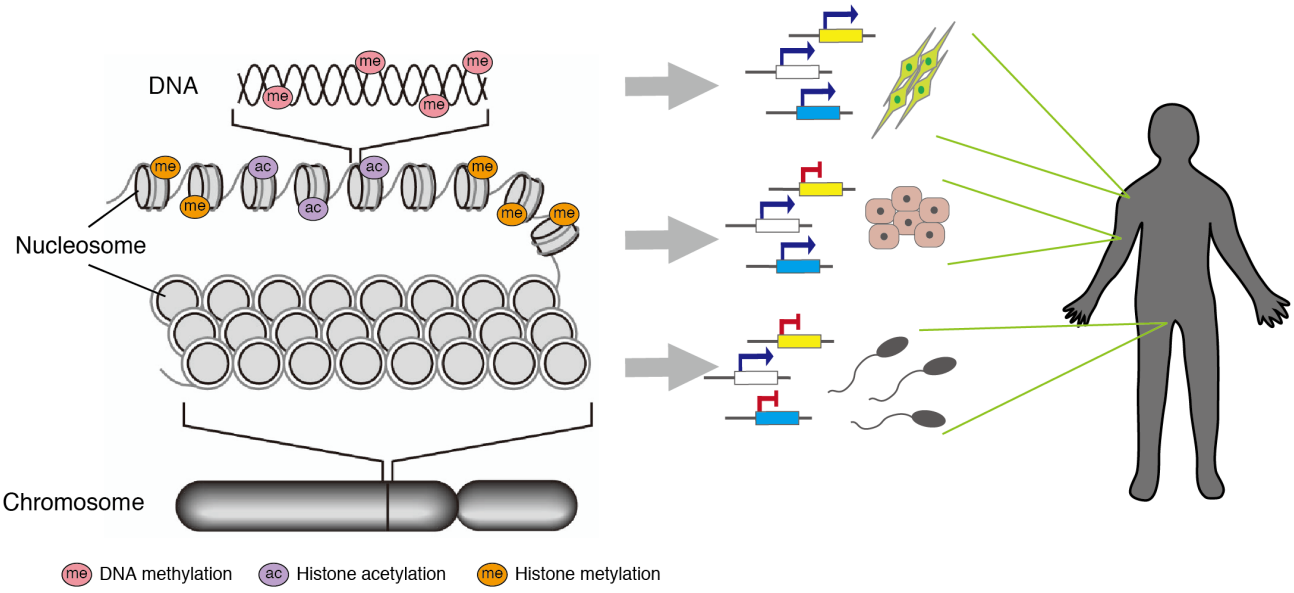

Figure 1. Epigenetic modification as a second layer of information associated with DNA

Epigenetic modification controls the establishment and maintenance of cellular identities for the entire life of multicellular organisms, sustaining proper organization of our whole body.

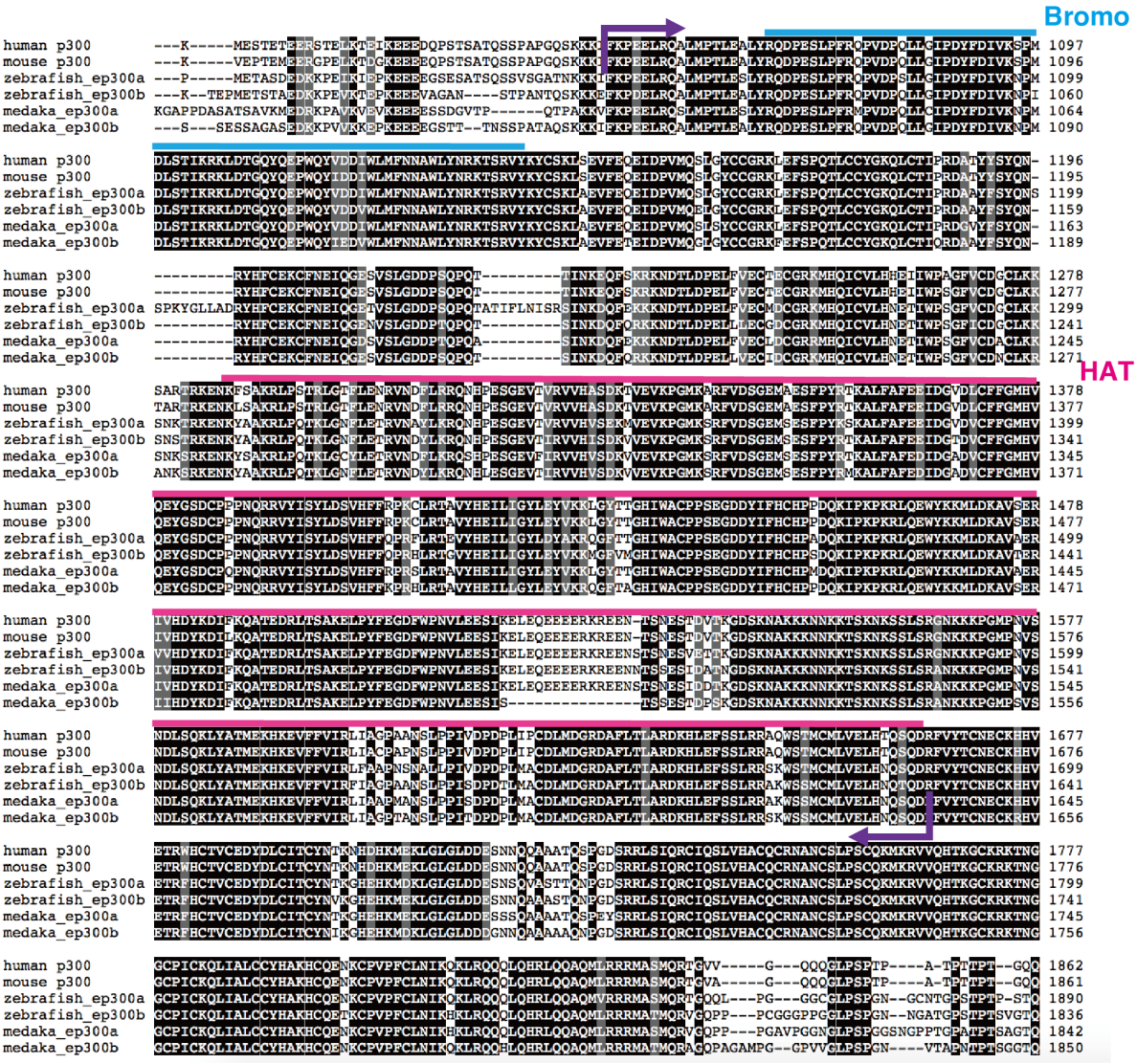

Figure 27. P300 core peptide alignment comparing human, mouse, zebrafish and medaka

Zebrafish and medaka have two p300 orthologs (ep300a and ep300b). The p300 core sequence is bracketed by purple arrows. The blue and magenta bars represent the Bromo domain and the HAT domain, respectively.

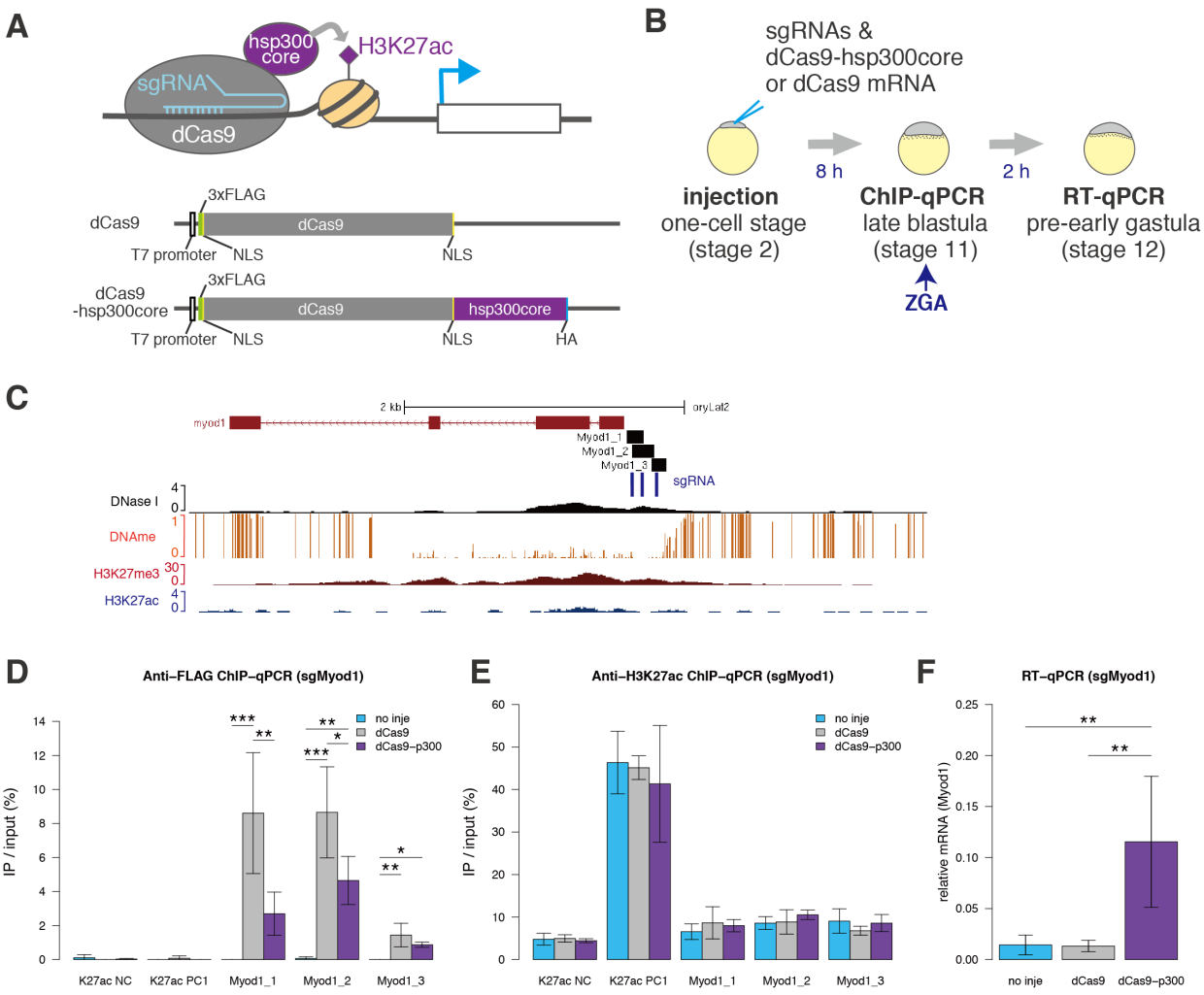

Figure 28. Figure legend on the next page

Figure 28. dCas9-hsp300core epigenome editing

(A) Schematic of dCas9 / dCas9-hsp300core constructs and H3K27ac induction / gene activation caused by dCas9-hsp300core.

(B) Schematic view of dCas9-hsp300core epigenome editing and injection experiments. sgRNA and mRNA were injected at the one-cell stage (stage 2). ChIP-qPCR was performed using the late blastula embryos (stage 11, eight hours after injection). RT-qPCR was performed using the pre-early gastrula embryos (stage 12, ten hours after injection), because ZGA occurs at the late blastula (stage 11) in medaka.

(C) The epigenetic modification pattern around the target Myod1, sgRNAs (blue bars) and ChIP-qPCR product (black bars) positions. H3K27me3 (red) and H3K27ac (blue) ChIP-seq, DNase I-seq (black) and DNA methylation enrichment at the blastula stage are shown.

(D, E) The results of ChIP-qPCR using anti-FLAG antibody and anti-H3K27ac antibody. H3K27ac negative region (K27ac NC) and H3K27ac positive region (K27ac PC1) were used for ChIP control (described in Figure 29). Light blue, gray, and purple bars represent no injection, sgRNAs / dCas9 injection and sgRNAs / dCas9-hsp300core injection, respectively.

(F) Myod1 mRNA expression level comparison by RT-qPCR. Expression levels were normalized to that of beta-actin. (Tukey-Kramer's test, * $p < 0.1$, ** $p < 0.05$, *** $p < 0.01$, n=3 biological replicates, error bars are s.d., p-values of each comparison are shown only if the p-value is under 0.1.)

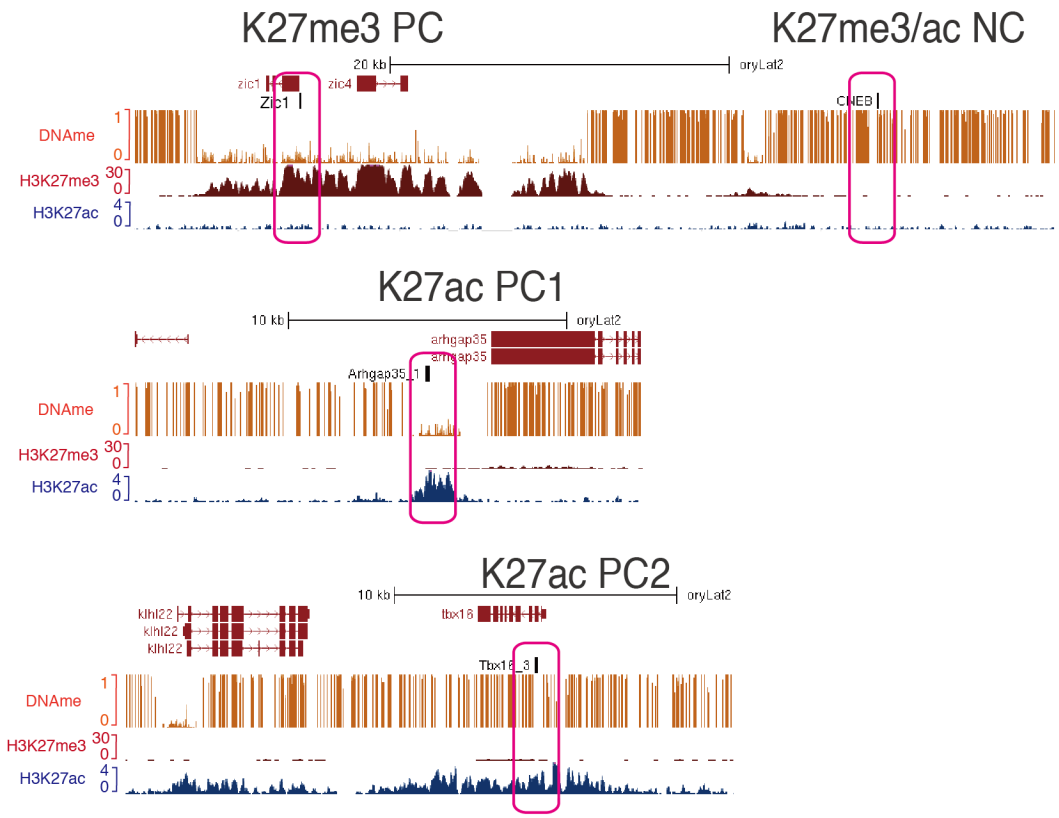

Figure 29. Location and epigenetic modification patterns of ChIP-qPCR negative control (NC) and positive control (PC)

H3K27me3 (red), H3K27ac (blue) enrichment (ChIP-seq)[30] and DNA methylation[29] at the blastula stage are shown. Black bars below the genes surrounded by magenta circles are the ChIP-qPCR product positions of each NC and PC.

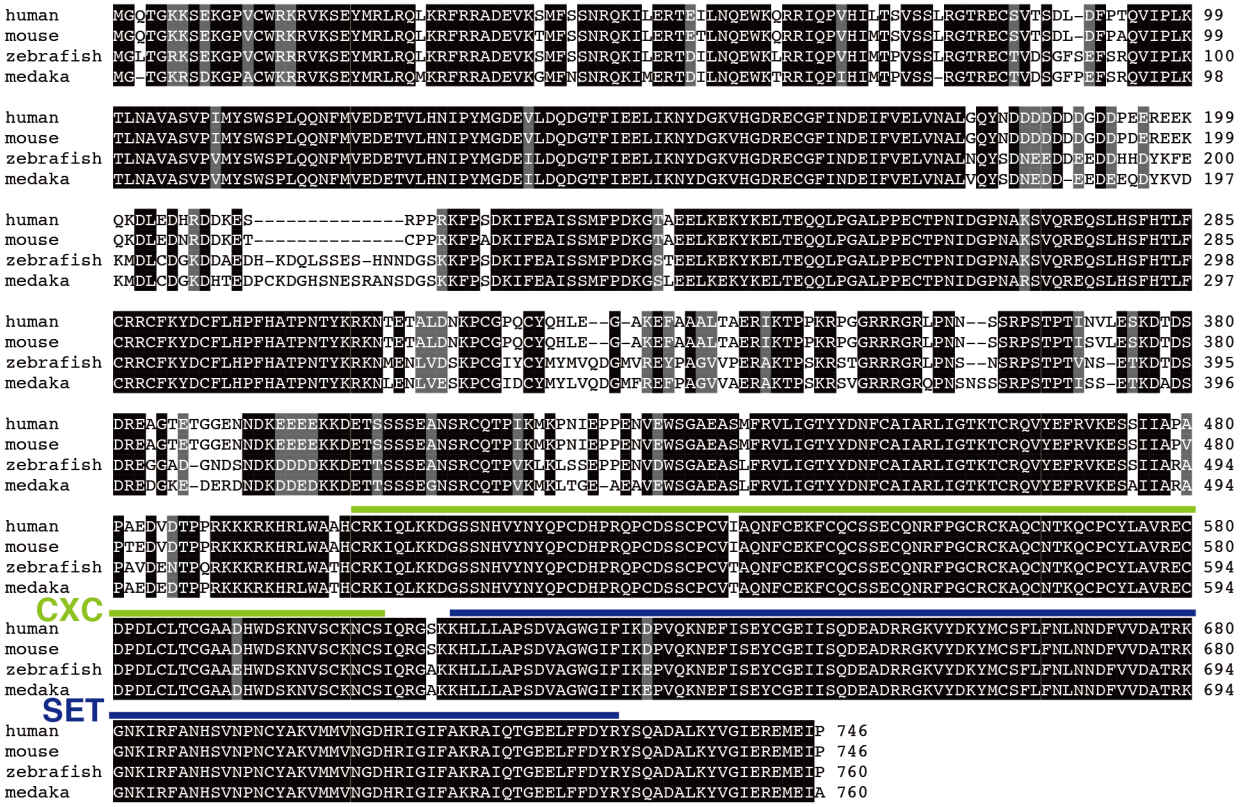

Figure 30. Ezh2 alignment comparing human, mouse, zebrafish and medaka

Alignment of Ezh2 protein sequences from four species. The green and blue bars indicate the CXC and the SET domains, respectively.

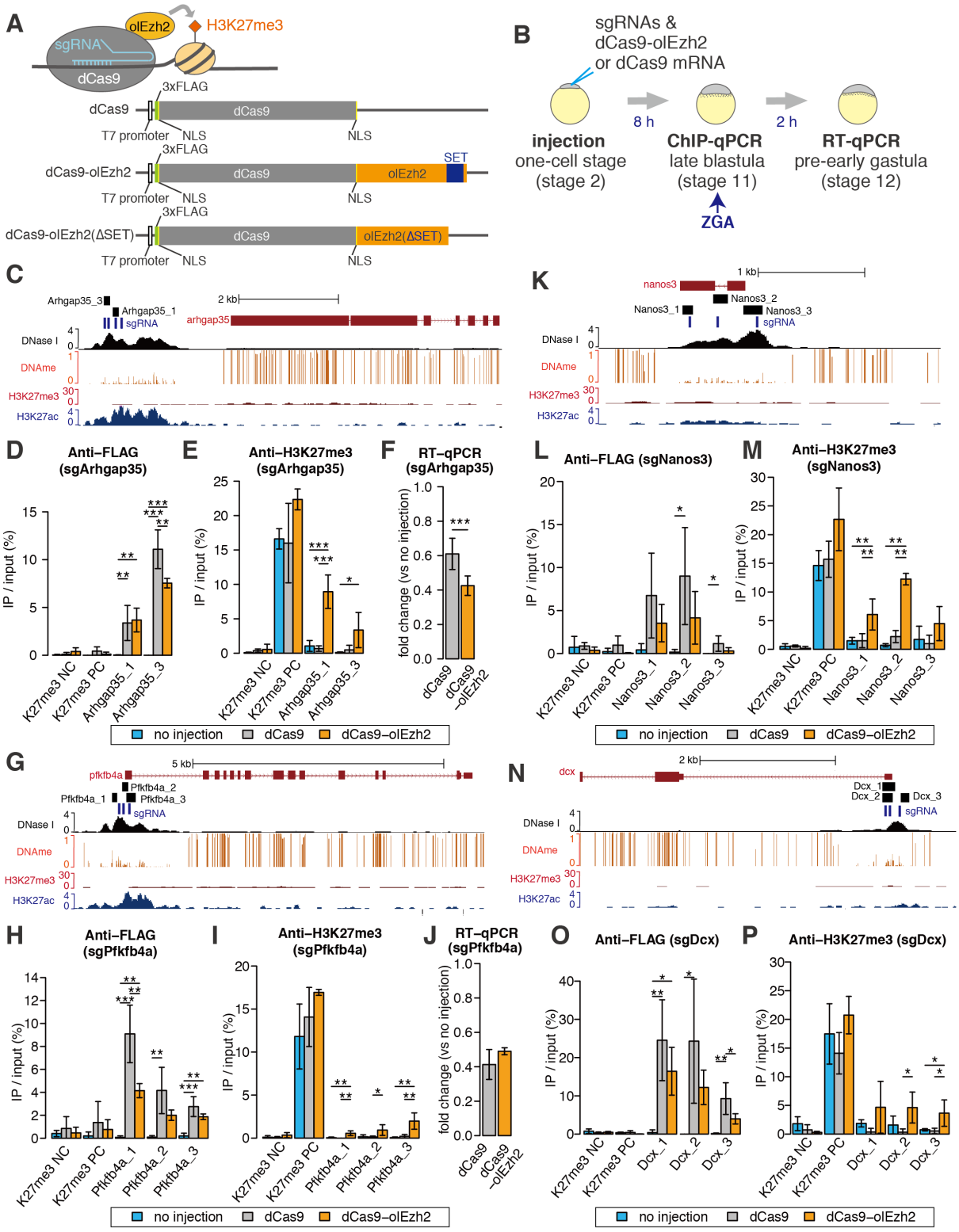

Figure 31. Figure legend on the next page

Figure 31. H3K27me3 epigenome editing by dCas9-olEzh2 targeting hypomethylated promoters

(A) Schematic of dCas9, dCas9-olEzh2 and dCas9-olEzh2(ΔSET) constructs and H3K27me3 induction caused by dCas9-olEzh2.

(B) Schematic view of the dCas9-olEzh2 epigenome editing and injection experiments. sgRNA and mRNA were injected at the one-cell stage (stage 2). ChIP-qPCR was performed using the late blastula embryos (stage 11, eight hours after injection). RT-qPCR was performed using the pre-early gastrula embryos (stage 12, ten hours after injection), because ZGA occurs at the late blastula (stage 11) in medaka.

(C, G, K, N) The epigenetic modification patterns around *Arhgap35, Kita*, *Nanos3* and *Dcx*, sgRNAs (blue bars) and ChIP-qPCR product (black bars) positions. H3K27me3 (red) and H3K27ac (blue) ChIP-seq[30], DNase I-seq (black)[63] and DNA methylation[29] enrichment at the blastula stage are shown.

(D, E, H, I, L, M, O, P) The results of ChIP-qPCR using anti-FLAG antibody (D, H, L, O) and anti-H3K27me3 antibody (E, I, L, M). H3K27me3 negative region (K27me3 NC) and H3K27me3 positive region (K27me3 PC) were used for ChIP control (described in Figure 29).

(F, J) *Arhgap35* and *Pfkfb4a* mRNA expression fold change. After expression levels were normalized to that of beta-actin, fold changes (sample / no injection) were calculated. Light blue, gray, and orange bars in each bar graph represent no injection, sgRNAs / dCas9 injection, and sgRNAs / dCas9-olEzh2 injection, respectively. (Tukey-Kramer test and only in Figure 31F, 31J Student's t-test, * $p < 0.1$, ** $p < 0.05$, *** $p < 0.01$, n=3 biological replicates and only in Figure 31F, 31J n=6 biological replicates, error bars are s.d., p-values of each comparison are shown only if the p-value is under 0.1.)

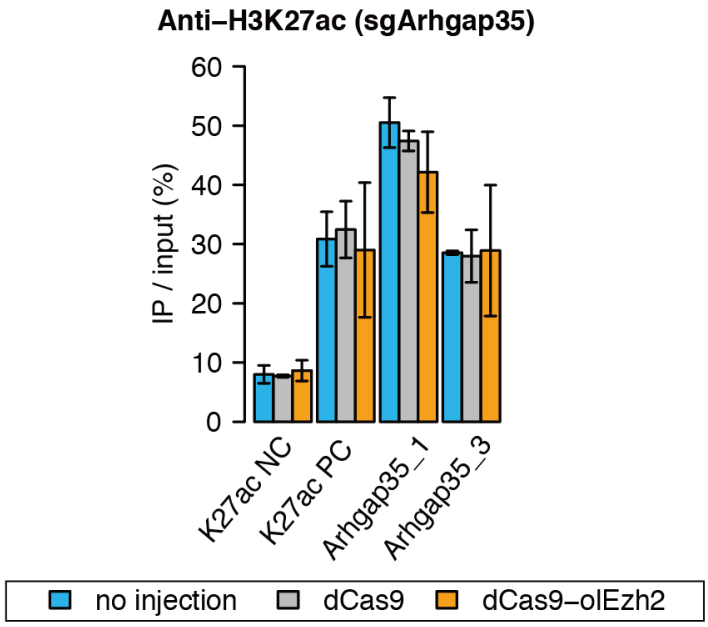

Figure 32. H3K27ac ChIP-qPCR of sgArhgap35 injected embryos

H3K27ac negative region (K27ac NC) and H3K27ac positive region (K27ac PC2) were used as controls for ChIP (described in Figure 29). Light blue, gray and orange bars represent no injection, sgRNAs / dCas9 injection and sgRNAs / dCas9-olEzh2 injection, respectively.

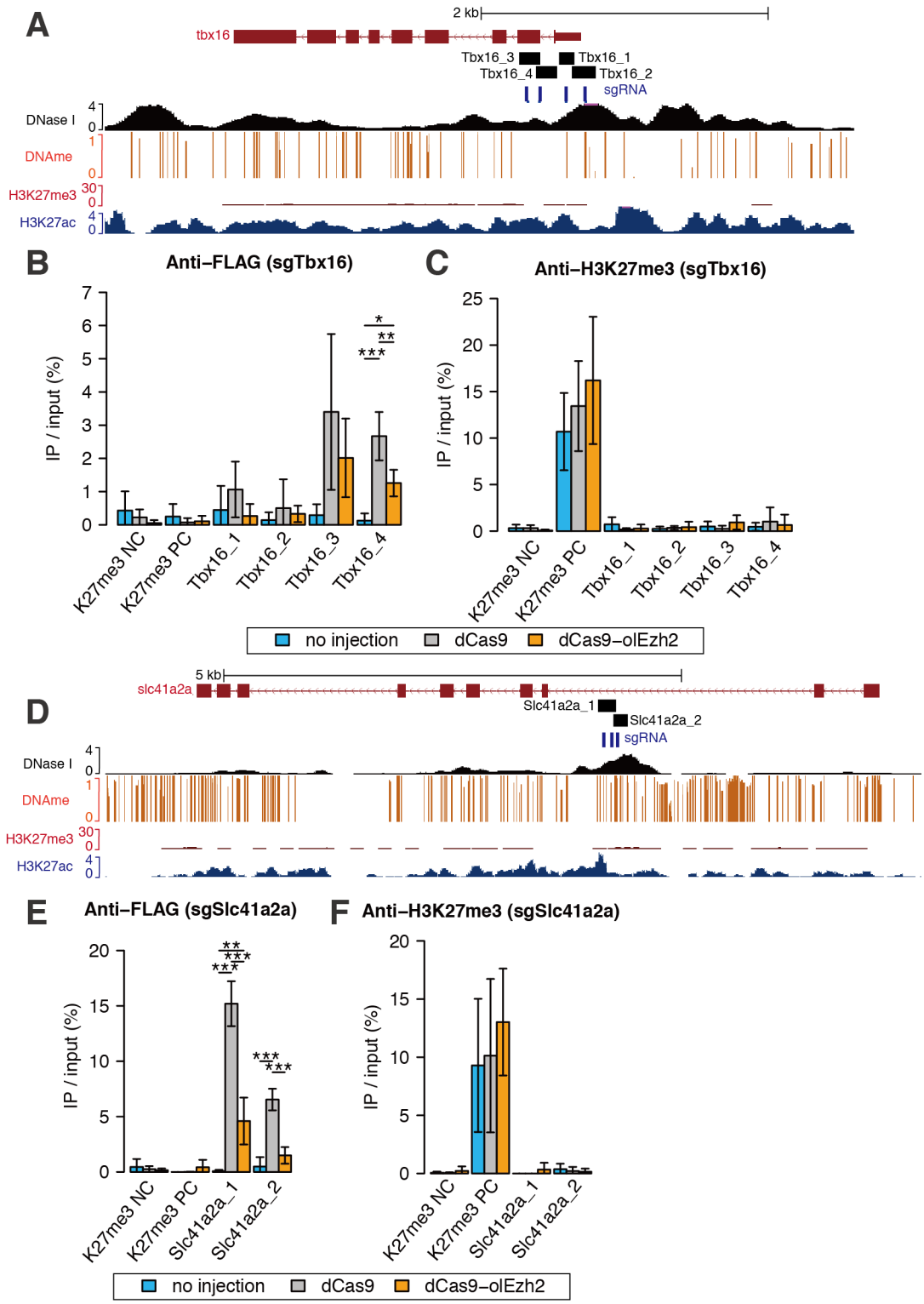

Figure 33. Figure legend on the next page

Figure 33. H3K27me3 epigenome editing by dCas9-olEzh2 targeting methylated promoters

(A, D) The epigenetic modification patterns around *Tbx16* and *Slc41a2a*, sgRNAs (blue bars) and ChIP-qPCR product (black bars) positions. H3K27me3 (red) and H3K27ac (blue) ChIP-seq[30], DNase I-seq (black)[63] and DNA methylation enrichment[29] at the blastula stage are shown for comparison.

(B, C, E, F) The results of ChIP-qPCR using anti-FLAG antibody (B, E) and anti-H3K27me3 antibody (C, F). H3K27me3 negative region (K27me3 NC) and H3K27me3 positive region (K27me3 PC) were used for ChIP control (described in Figure 29). Light blue, gray, and orange bars represent no injection, sgRNAs / dCas9 injection, and sgRNAs / dCas9-olEzh2 injection, respectively. (Tukey-Kramer test, * $p < 0.1$, ** $p < 0.05$, *** $p < 0.01$, n=3 biological replicates, error bars are s.d., p-values of each comparison are shown only if the p-value is under 0.1.)

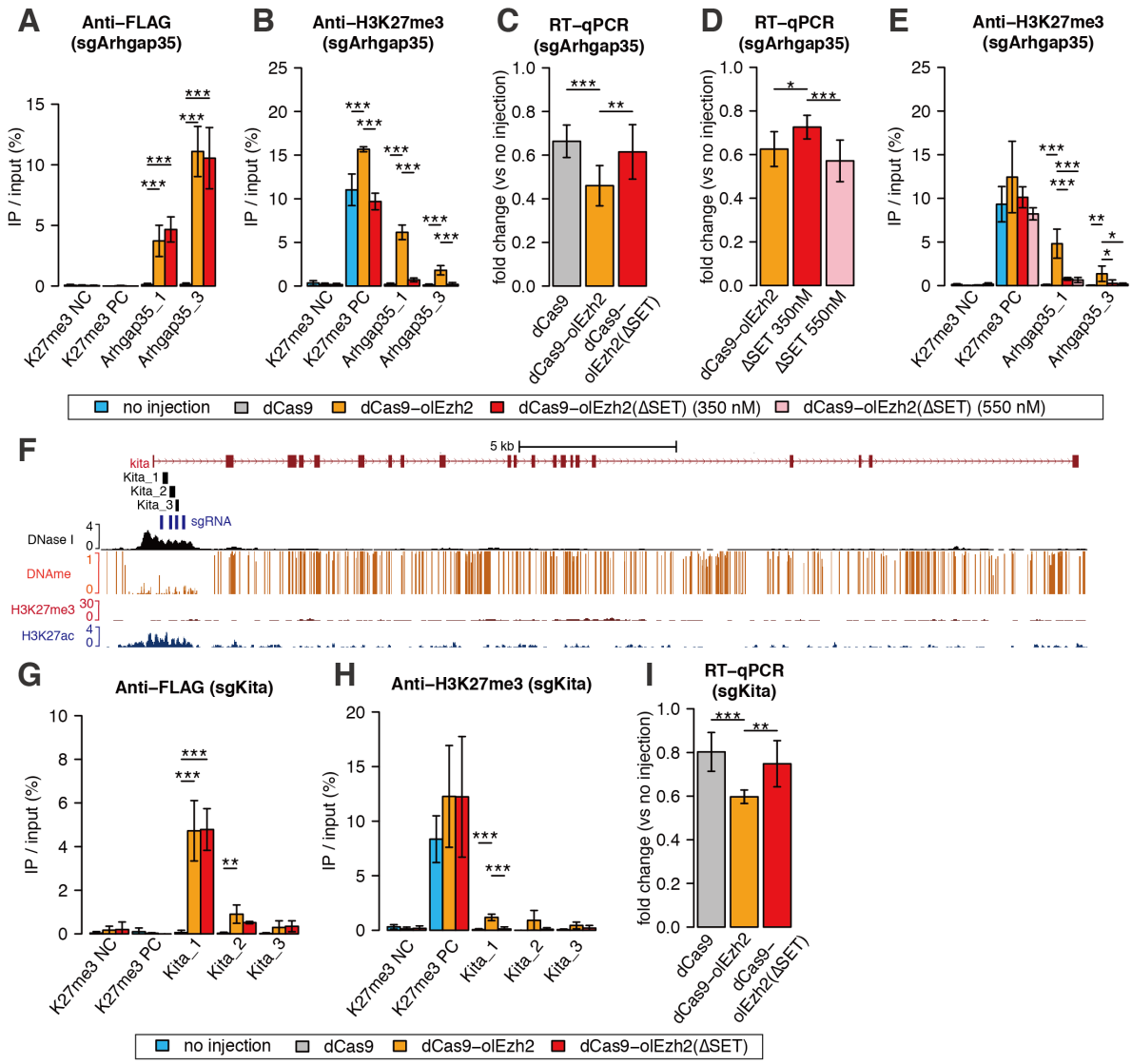

Figure 34. Figure legend on the next page

Figure 34. H3K27me3 epigenome editing by dCas9-olEzh2(ΔSET) and higher concentration injection

(A-C) dCas9-olEzh2(ΔSET) analyses targeting *Arhgap35* promoter. ChIP-qPCR using anti-FLAG antibody (A), ChIP-qPCR using anti-H3K27me3 antibody (B), and *Arhgap35* mRNA expression fold change (C).

(D, E) Arhgap35 mRNA expression fold change (D) and ChIP-qPCR using anti-H3K27me3 antibody (E) in higher concentration injection.

(F) The epigenetic modification patterns around *Kita*, sgRNAs (blue bars) and ChIP-qPCR product (black bars) positions. H3K27me3 (red) and H3K27ac (blue) ChIP-seq[30], DNase I-seq (black)[63] and DNA methylation enrichment[29] at the blastula stage are shown for comparison.

(G-I) dCas9-olEzh2(ΔSET) analyses targeting *Kita* promoter. ChIP-qPCR using anti-FLAG antibody (g), ChIP-qPCR using anti-H3K27me3 antibody (H), and *Kita* mRNA expression fold change (I).

In Figure 34C, 34D and 34I, after expression levels were normalized to that of beta-actin, fold changes (sample / no injection) were calculated. Light blue, gray, orange, red and pink bars in each bar graph represent no injection, sgRNAs / dCas9 injection, sgRNAs / dCas9-olEzh2 injection, sgRNAs / dCas9-olEzh2(ΔSET)(350nM) injection, and sgRNAs / dCas9-olEzh2(ΔSET)(550nM) injection respectively. (Tukey-Kramer test, * $p < 0.1$, ** $p < 0.05$, *** $p < 0.01$, n=3 biological replicates and only in Figure 34C, 34D and 34I n=6 biological replicates, error bars are s.d., p-values of each comparison are shown only if the p-value is under 0.1.)

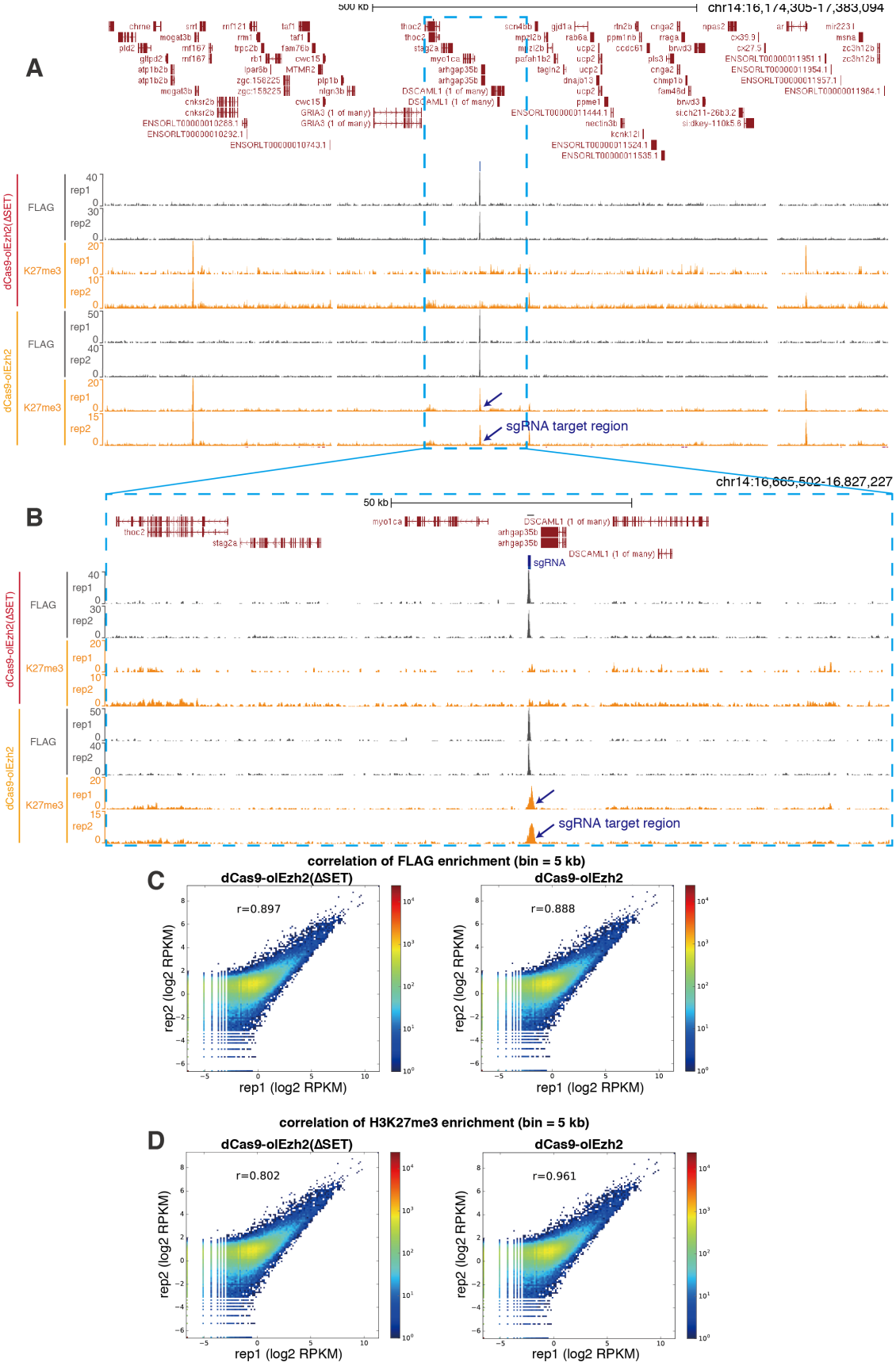

Figure 35. Figure legend on the next page

Figure 35. Comparison between two biological replicates of ChIP-seq

(A, B) Genome browser view of ChIP-seq for each biological replicate. Induced H3K27me3 accumulation at the target locus is indicated by arrows.

(C, D) Correlation of two ChIP-seq replicates. Log2(RPKM) of each bins (5kb) and Pearson's correlation coefficient are shown.

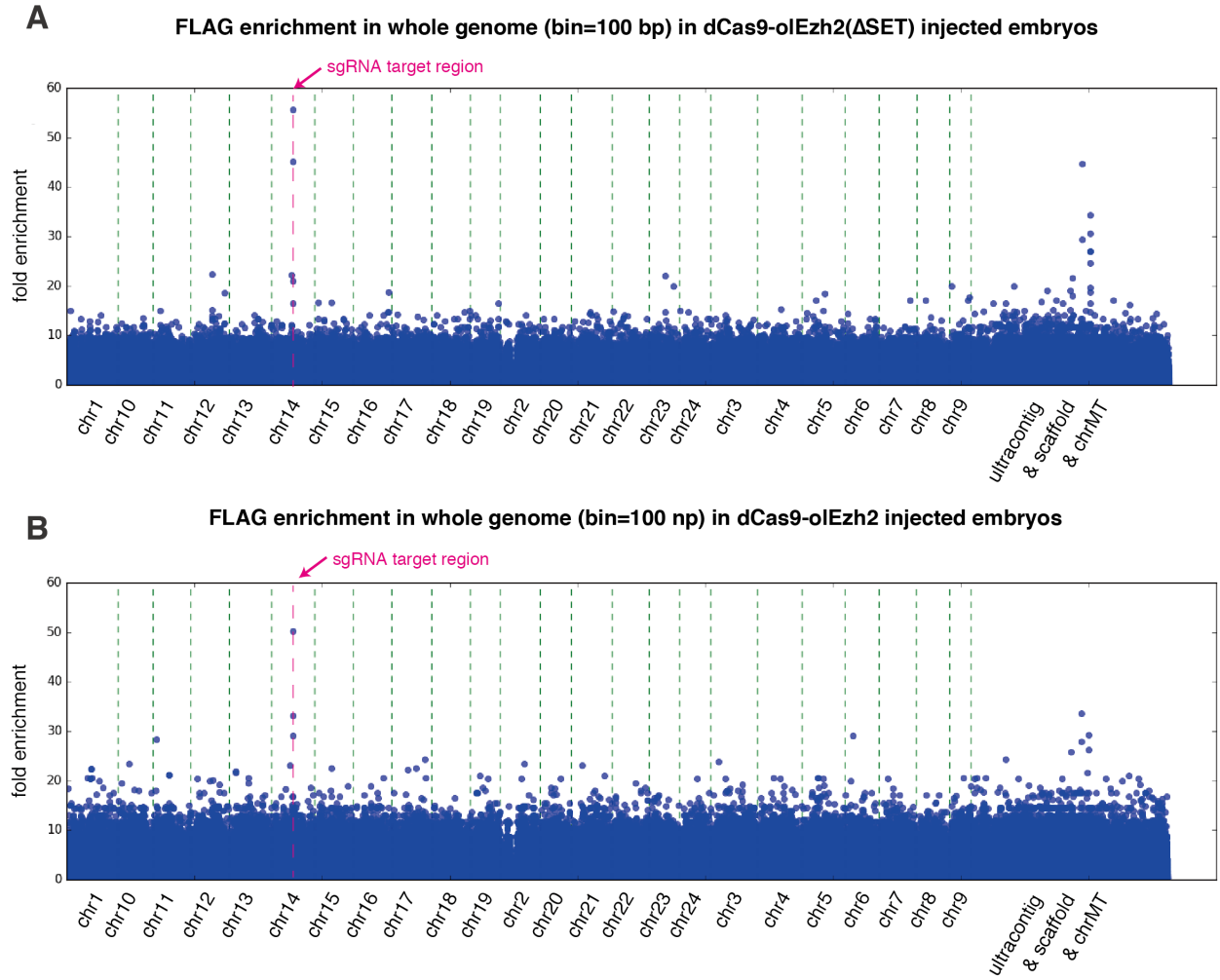

Figure 36. Genome-wide distribution of FLAG ChIP-seq signal

(A, B) Fold enrichment of FLAG ChIP-seq signal for (A) dCas9-olEzh2(ΔSET) injected embryos and (B) dCas9-olEzh2 injected embryos. The position of sgRNA target site is indicated by magenta line.

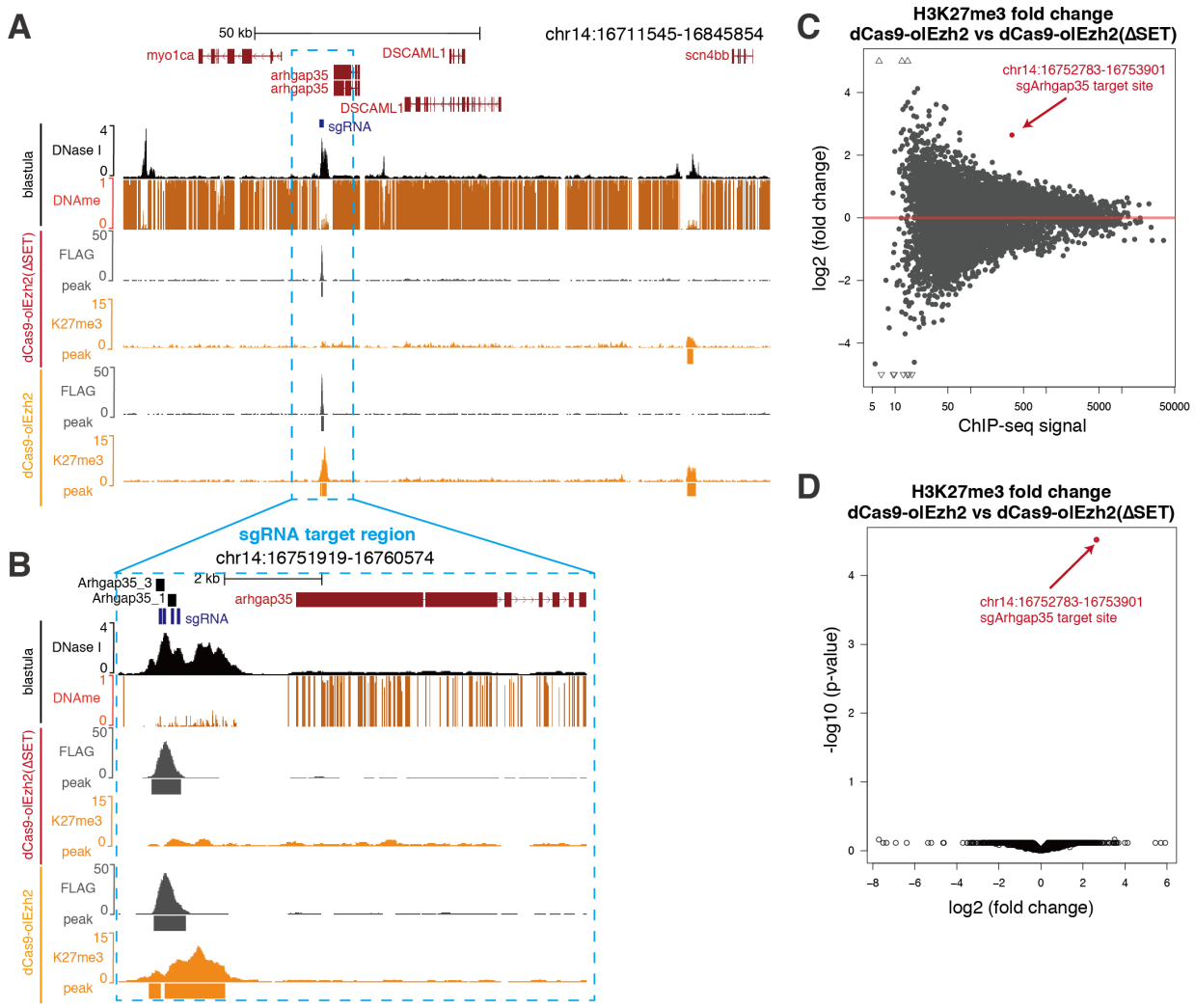

Figure 37. H3K27me3 epigenome editing was highly site-specific

(A, B) Epigenetic modification patterns, sgRNAs (blue bars) and ChIP-qPCR product (black bars) positions around sgRNA target site. ChIP-seq using anti-FLAG antibody (gray) and anti-H3K27me3 (orange) in dCas9-olEzh2(SET) or dCas9-olEzh2 injected embryos are shown. In addition, DNase I-seq (black)[63] and DNA methylation[29] pattern of blastula stage are shown.

(C) MA plot of differential enrichment analysis of ChIP-seq signals of dCas9-olEzh2(SET) injected embryos and dCas9-olEzh2 injected embryos. Each dot shows H3K27me3 peak. The peak with the p-value under 0.01 is indicated as red dot. The peaks with the fold change greater than 5 or less than -5 are indicated as triangles.

(D) Volcano plot of differential enrichment analysis of ChIP-seq signals of dCas9-olEzh2(SET) injected embryos and dCas9-olEzh2 injected embryos. All H3K27me3 peaks are indicated as dots. Only the peak including targeted genomic region is indicated as red dot.

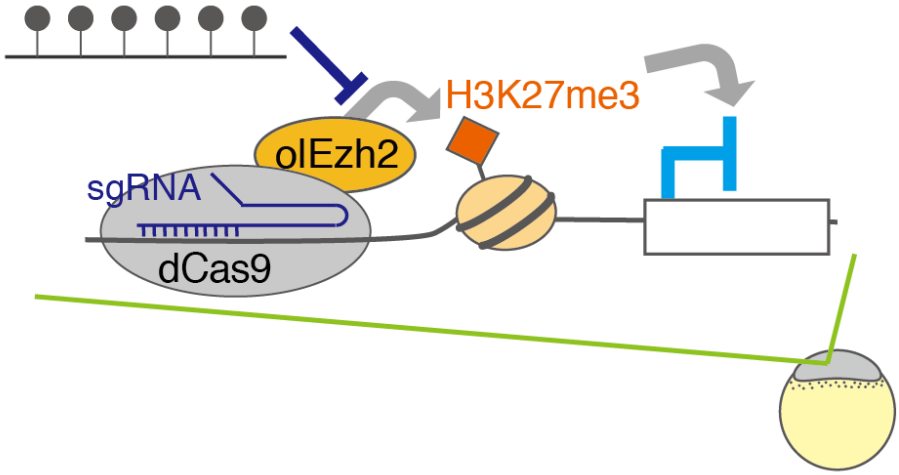

Figure 38. Summary of Chapter 2

The new construct dCas9-olEzh2 can induce H3K27me3 site-specifically and cause significant reduction of expression level of downstream gene. This activity is inhibited by pre-existing DNA methylation.

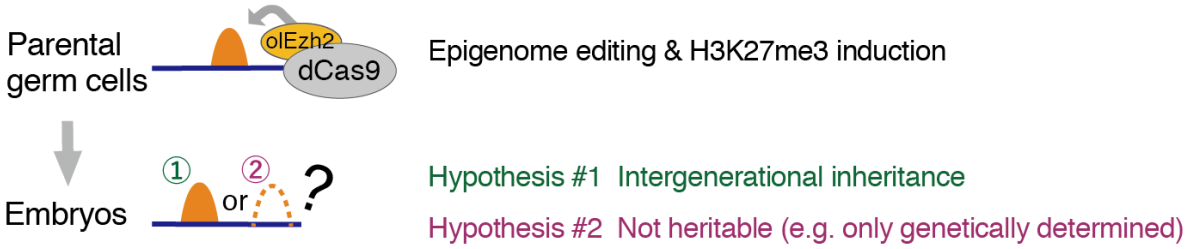

Figure 39. Future study for testing intergenerational inheritance of histone modifications.

If H3K27me3 (orange) can be heritable intergenerationally, H3K27me3 accumulation induced by epigenome editing in parental germ cells causes H3K27me3 accumulation in embryos at the same genomic region. If not (e.g. H3K27me3 deposition in embryos are determined by DNA-sequence alone), such artificial induction of H3K27me3 in parental germ cells do not cause H3K27me3 accumulation in embryos.

Tables

Table S1. sgRNA targets

name	sgRNA target (18bp) + NGG	location
sgArhgap35_1	ACCACACGATAGCGCCTCTGG	chr14:16752902-16752922
sgArhgap35_2	TGCCGACATAATAACGCTGGG	chr14:16753019-16753039
sgArhgap35_3	ATGTGGAATCGATTACTTTGG	chr14:16752685-16752705
sgArhgap35_4	TTGTGTGAGGGCGCCGCTGGG	chr14:16752757-16752777
sgPfkfb4a_1	CGCGCGAGCGCTACCGACTGG	chr5:25992580-25992600
sgPfkfb4a_2	TACACAGTCACCGACACGGGG	chr5:25992672-25992692
sgPfkfb4a_3	GGGAAGCCCGTTTTTATACGG	chr5:25992789-25992809
sgTbx16_1	ACTCAATGTGTAATCCGTGGG	chr9:20564664-20564684
sgTbx16_2	GGTGGACGACGACTTTTAAGG	chr9:20564800-20564820
sgTbx16_3	CTGGAGGATCCCAACCTCTGG	chr9:20564401-20564421
sgTbx16_4	GAGGAGGGCCACTGAAGTTGG	chr9:20564478-20564498
sgSlc41a2a_1	GAGTCGTTGCAATCGTCTGGG	chr6:26429286-26429306
sgSlc41a2a_2	ACAGATTTAGTGTAGTCGAGG	chr6:26429140-26429160
sgSlc41a2a_3	AGCTCGAATCCCTTCTAGTGG	chr6:26429232-26429252
sgNanos3_1	GGGCACACGTACTGCCGCAGG	chr1:31476661-31476681
sgNanos3_2	CTTCGTGCACCCCCGCTCCGG	chr1:31476915-31476935
sgNanos3_3	GCGCGTGCACAGCGCGTGCGG	chr1:31477286-31477306
sgDcx_1	CACCTGCGCGGCTGCGTGCGG	chr14:14993085-14993105
sgDcx_2	CGGTGCGGTGCGGGGGAAGGG	chr14:14993121-14993141
sgDcx_3	GACTCGCACCTCCGCGGTGGG	chr14:14993297-14993317
sgKita_1	ACTCCGGGCTCTCTTAACCGG	chr4:1430456-1430476
sgKita_2	ACATAACCGTCACTATCATGG	chr4:1430718-1430738
sgKita_3	TCAGGTACATAATATACGAGG	chr4:1430924-1430944

sgKita_4	GTCATGAAAAGCCACTTCAGG	chr4:1431112-1431132

Table S2. Primers and oligos

name	purpose	Primer Sequence (5'->3')
olEzh2 F	cloning olEzh2	TGGCTGCAGGCTGATCAT
olEzh2 R	cloning olEzh2	TCAGGCGATCTCCATCTC
mut.1_F	dCas9 mutagenesis (D10A)	GGCTTAGCTATCGGCACAAATAGCGT
mut.1_R	dCas9 mutagenesis (D10A)	GCCGATAGCTAAGCCTATTGAGTATT
mut.2_F	dCas9 mutagenesis (H840A)	TGTCGATGCCATTGTTCCACAAAGTTT
mut.2_R	dCas9 mutagenesis (H840A)	ACAATGGCATCGACATCATAATCACT
NEBuilder dCas9 F	make pCS2+-dCas9	ATACGACTCACTATAGTTGAGAGCCGCCACCATGGAC
NEBuilder dCas9 R	make pCS2+-dCas9	AGGCCTCTCGAGCCTAAACTCAATGGTGATGGTGATGAT GACC
NEBuilder olezh2 F	make pCS2+-dCas9-olEzh2	CCCAAGAAGAAGAGGAAAGTCCGCGCCGGGACGGGGA AACGCTCAG
NEBuilder olezh2 R	make pCS2+-dCas9-olEzh2	TCGAATTCAAGGCCTCTCAGGCGATCTCCATCTCGC
mut-olEzh2-ΔSET F	make Ezh2(ΔSET)	AGCCAAGTACAGCCAGGCGGACGCC
mut-olEzh2-ΔSET R	make Ezh2(ΔSET)	TGGCTGTACTTGGCTCCTCTCTGGAT
IVT dCas9-olezh2 F	IVT template (dCas9 or dCas9-olEzh2)	GGATCTACGTAATACGACTCACTA
IVT dCas9-olezh2 R	IVT template (dCas9 or dCas9-olEzh2)	GCTACTTGTTCTTTTTGCAGG

IVT sgRNA F	IVT template (sgRNA)	AAAAGCACCGACTCGGTG
IVT sgRNA R	IVT template (sgRNA)	GGTCAGGTATGATTTAAATGGTCAGT
sgArhgap35_1s	sgRNA oligo	TAGGACCACACGATAGCGCCTC
sgArhgap35_1a	sgRNA oligo	AAACGAGGCGCTATCGTGTGGT
sgArhgap35_2s	sgRNA oligo	TAGGTGCCGACATAATAACGCT
sgArhgap35_2a	sgRNA oligo	AAACAGCGTTATTATGTCGGCA
sgArhgap35_3s	sgRNA oligo	TAGGATGTGGAATCGATTACTT
sgArhgap35_3a	sgRNA oligo	AAACAAGTAATCGATTCCACAT
sgArhgap35_4s	sgRNA oligo	TAGGTTGTGTGAGGGCGCCGCT
sgArhgap35_4a	sgRNA oligo	AAACAGCGGCGCCCTCACACAA
sgPfkfb4a_1s	sgRNA oligo	TAGGCGCGCGAGCGCTACCGAC
sgPfkfb4a_1a	sgRNA oligo	AAACGTCGGTAGCGCTCGCGCG
sgPfkfb4a_2s	sgRNA oligo	TAGGTACACAGTCACCGACACG
sgPfkfb4a_2a	sgRNA oligo	AAACCGTGTCGGTGACTGTGTA
sgPfkfb4a_3s	sgRNA oligo	TAGGGGGAAGCCCGTTTTTATA
sgPfkfb4a_3a	sgRNA oligo	AAACTATAAAAACGGGCTTCCC
sgTbx16_1s	sgRNA oligo	TAGGACTCAATGTGTAATCCGT
sgTbx16_1a	sgRNA oligo	AAACACGGATTACACATTGAGT
sgTbx16_2s	sgRNA oligo	TAGGGGTGGACGACGACTTTTA
sgTbx16_2a	sgRNA oligo	AAACTAAAAGTCGTCGTCCACC
sgTbx16_3s	sgRNA oligo	TAGGCTGGAGGATCCCAACCTC
sgTbx16_3a	sgRNA oligo	AAACGAGGTTGGGATCCTCCAG
sgTbx16_4s	sgRNA oligo	TAGGGAGGAGGGCCACTGAAGT
sgTbx16_4a	sgRNA oligo	AAACACTTCAGTGGCCCTCCTC
sgSlc41a2a_1s	sgRNA oligo	TAGGGAGTCGTTGCAATCGTCT
sgSlc41a2a_1a	sgRNA oligo	AAACAGACGATTGCAACGACTC

sgSlc41a2a_2s	sgRNA oligo	TAGGACAGATTTAGTGTAGTCG
sgSlc41a2a_2a	sgRNA oligo	AAACCGACTACACTAAATCTGT
sgSlc41a2a_3s	sgRNA oligo	TAGGAGCTCGAATCCCTTCTAG
sgSlc41a2a_3a	sgRNA oligo	AAACCTAGAAGGGATTCGAGCT
sgNanos3_1s	sgRNA oligo	TAGGGGGCACACGTACTGCCGC
sgNanos3_1a	sgRNA oligo	AAACGCGGCAGTACGTGTGCCC
sgNanos3_2s	sgRNA oligo	TAGGCTTCGTGCACCCCCGCTC
sgNanos3_2a	sgRNA oligo	AAACGAGCGGGGGTGCACGAAG
sgNanos3_3s	sgRNA oligo	TAGGGCGCGTGCACAGCGCGTG
sgNanos3_3a	sgRNA oligo	AAACCACGCGCTGTGCACGCGC
sgDcx_1s	sgRNA oligo	TAGGACCTGCGCGGCTGCGTGC
sgDcx_1a	sgRNA oligo	AAACGCACGCAGCCGCGCAGGT
sgDcx_2s	sgRNA oligo	TAGGCGGTGCGGTGCGGGGGAA
sgDcx_2a	sgRNA oligo	AAACTTCCCCCGCACCGCACCG
sgDcx_3s	sgRNA oligo	TAGGGACTCGCACCTCCGCGGT
sgDcx_3a	sgRNA oligo	AAACACCGCGGAGGTGCGAGTC
sgKita_1s	sgRNA oligo	TAGGACTCCGGGCTCTCTTAAC
sgKita_1a	sgRNA oligo	AAACGTTAAGAGAGCCCGGAGT
sgKita_2s	sgRNA oligo	TAGGACATAACCGTCACTATCA
sgKita_2a	sgRNA oligo	AAACTGATAGTGACGGTTATGT
sgKita_3s	sgRNA oligo	TAGGTCAGGTACATAATATACG
sgKita_3a	sgRNA oligo	AAACCGTATATTATGTACCTGA
sgKita_4s	sgRNA oligo	TAGGGTCATGAAAAGCCACTTC
sgKita_4a	sgRNA oligo	AAACGAAGTGGCTTTTCATGAC

Table S3. ChIP-qPCR primers

name	Forward Primer Sequence (5'->3')	Reverse Primer Sequence (5'->3')	location
Arhgap35_1	AGAGGAGATCTCGGTCCAGG	CGTGCCGTTTCCTTCCAAAT	chr14:16752834-16752975
Arhgap35_3	ACAAGCTCTCGTGGATGTGG	ACACAAGCAACGGAGAGAGG	chr14:16752671-16752803
Pfkfb4a_1	GTTGATGGGCCTGTCCCAAA	GATGTTTCCCGTGATGCTGC	chr5:25992515-25992672
Pfkfb4a_2	GCAGCATCACGGGAAACATC	GGGTGAGTTCGCGATGAGTA	chr5:25992653-25992762
Pfkfb4a_3	GCCTCTACTCATCGCGAACT	CCAGCTACACAAGACAAAGGC	chr5:25992738-25992922
Tbx16_1	CAGCAGCTCTGGCTGAGAAA	CTTTCACACTTGAGGCAGGC	chr9:20564630-20564731
Tbx16_2	GCCTGCCTCAAGTGTGAAAG	GGCTCATCACCGTGTCACTT	chr9:20564712-20564886
Tbx16_3	ACCTGCCTGGCTTTGTGATA	CAACTTCAGTGGCCCTCCTC	chr9:20564349-20564497
Tbx16_4	CAGTGATGGCAGTGGGAGG	TGCAGTCCATCAGAGGTGAG	chr9:20564463-20564615
Slc41a2a_1	CCTGCTGGTCGCCACATTTA	CGACTCTGAAGGCGTCAACA	chr6:26429104-26429291
Slc41a2a_2	GGTGTTGACGCCTTCAGAGT	CTACGCCACCACCTATCTCC	chr6:26429270-26429412

Nanos3_1	AGTTCTGTCCACCTTCGGAC	TGTGTTGTGTCCCTACCTGC	chr1:31476597-31476696
Nanos3_2	CAAAGCTACCTGGGAGATGGG	GGGCCATCGTTCAAGCAAAT	chr1:31476881-31477020
Nanos3_3	GACATGCTTAGCGCACCTCT	CGTCACGCTTCACCTGTTCA	chr1:31477165-31477345
Dcx_1	TAGGAGAATAGGAGTCATGTGGTTT	GAAGCAGACAAAGGCAGAGC	chr14:14993043-14993224
Dcx_2	AGGAGAATAGGAGTCATGTGGTTT	CGCTATCCTTCCTGCTGCAT	chr14:14993044-14993189
Dcx_3	GGAGGTGCGAGTCTGCG	CAGCCACCACAGCAATTCAT	chr14:14993305-14993422
Zic1	CATCAGATGAGCGTTGTAGG	CTGAGACGACTGAGAGCAG	chr20:16773372-16773539
CNEB	ACGCTGCATGCATCAAACAAGGC	TGTCACACAACCCGGGCACAC	chr20:16807468-16807603
Kita_1	CCCGGAGTAACGAAACCCAA	ATTCTGACCTGTCGGCTTCC	chr4:1430469-1430657
Kita_2	AGCTCCTGCTGTCCCTACAT	CATGAATGACCTCTGCGGGT	chr4:1430702-1430899
Kita_3	CCGCAGAGGTCATTCATGGT	ACGTCCATGTTTCCTGACTCC	chr4:1430882-1431010

Table S4. RT-qPCR primers

name	Forward Primer Sequence (5'->3')	Reverse Primer Sequence (5'->3')
Arhgap35	TGAAGAGCCTCAGACGAACAG	TACGCGGTACAAACCCTCTG
Pfkfb4a	CATCGCGAACTCACCCAGAA	CCGATCCAGTTCAGGTAGCG
beta-actin	TGCCGCACTGGTTGTTGACAACG	CCATGACACCCTGGTGCCTGG
Kita	AGCAACAGCTGTCAGACTCC	GGAGCAGTAAGGGCTGTGTT

References

1. Miska, E. A. & Ferguson-Smith, A. C. Transgenerational inheritance: Models and mechanisms of non-DNA sequence-based inheritance. *Science* **354**, 59–63 (2016).
2. Danchin, É. *et al.* Beyond DNA: Integrating inclusive inheritance into an extended theory of evolution. *Nature Reviews Genetics* vol. 12 475–486 (2011).
3. GURDON, J. B. The developmental capacity of nuclei taken from intestinal epithelium cells of feeding tadpoles. *J. Embryol. Exp. Morphol.* **10**, (1962).
4. Thakore, P. I., Black, J. B., Hilton, I. B. & Gersbach, C. A. Editing the epigenome: technologies for programmable transcription and epigenetic modulation. *Nat. Methods* **13**, 127–137 (2016).
5. Zhou, V. W., Goren, A. & Bernstein, B. E. Charting histone modifications and the functional organization of mammalian genomes. *Nat. Rev. Genet.* **12**, 7–18 (2011).
6. Greenberg, M. V. C. & Bourc'his, D. The diverse roles of DNA methylation in mammalian development and disease. *Nat. Rev. Mol. Cell Biol.* **20**, 590–607 (2019).
7. Reinberg, D. & Vales, L. D. Chromatin domains rich in inheritance. *Science (80-.).* **361**, 33–34 (2018).
8. Henikoff, S. & Greally, J. M. Epigenetics, cellular memory and gene regulation. *Current Biology* vol. 26 R644–R648 (2016).
9. D'Urso, A. & Brickner, J. H. Mechanisms of epigenetic memory. *Trends in Genetics* vol. 30 230–236 (2014).
10. Gangisetty, O. & Murugan, S. Epigenetic Modifications in Neurological Diseases: Natural Products as Epigenetic Modulators a Treatment Strategy. in 1–25 (2016). doi:10.1007/978-3-319-28383-8_1.
11. Heard, E. & Martienssen, R. A. Transgenerational epigenetic inheritance: Myths and mechanisms. *Cell* vol. 157 95–109 (2014).
12. Perez, M. F. & Lehner, B. Intergenerational and transgenerational epigenetic inheritance in animals. *Nat. Cell Biol.* **21**, 143–151 (2019).
13. Jablonka, E. & Raz, G. Transgenerational Epigenetic Inheritance: Prevalence, Mechanisms, and Implications for the Study of Heredity and Evolution. *Q. Rev. Biol.* **84**, 131–176 (2009).
14. Landman, O. E. The Inheritance of Acquired Characteristics. *Annu. Rev. Genet.* **25**, 1–20 (1991).
15. Veenendaal, M. *et al.* Transgenerational effects of prenatal exposure to the 1944-45 Dutch famine. *BJOG An Int. J. Obstet. Gynaecol.* **120**, 548–554 (2013).

16. Waterland, R. A. & Jirtle, R. L. Transposable Elements: Targets for Early Nutritional Effects on Epigenetic Gene Regulation. *Mol. Cell. Biol.* **23**, 5293–5300 (2003).
17. Duhl, D. M. J., Vrieling, H., Miller, K. A., Wolff, G. L. & Barsh, G. S. Neomorphic agouti mutations in obese yellow mice. *Nat. Genet.* **8**, 59–65 (1994).
18. Tobi, E. W. *et al.* DNA methylation signatures link prenatal famine exposure to growth and metabolism. *Nat. Commun.* **5**, 5592 (2014).
19. Feder, A., Nestler, E. J. & Charney, D. S. Psychobiology and molecular genetics of resilience. *Nat. Rev. Neurosci.* **10**, 446–457 (2009).
20. Manning, K. *et al.* A naturally occurring epigenetic mutation in a gene encoding an SBP-box transcription factor inhibits tomato fruit ripening. *Nat. Genet.* **38**, 948–952 (2006).
21. Cubas, P., Vincent, C. & Coen, E. An epigenetic mutation responsible for natural variation in floral symmetry. *Nature* **401**, 157–161 (1999).
22. Teperek, M. *et al.* Sperm is epigenetically programmed to regulate gene transcription in embryos. *Genome Res.* **26**, 1034–1046 (2016).
23. Siklenka, K. *et al.* Disruption of histone methylation in developing sperm impairs offspring health transgenerationally. *Science (80-.).* **350**, aab2006–aab2006 (2015).
24. Lesch, B. J. *et al.* Intergenerational epigenetic inheritance of cancer susceptibility in mammals. *Elife* **8**, (2019).
25. Morgan, M. A. J. & Shilatifard, A. Reevaluating the roles of histone-modifying enzymes and their associated chromatin modifications in transcriptional regulation. *Nat. Genet.* **52**, 1271–1281 (2020).
26. Xia, W. & Xie, W. Rebooting the Epigenomes during Mammalian Early Embryogenesis. *Stem Cell Reports* **15**, 1158–1175 (2020).
27. Fukushima, H. S., Takeda, H. & Nakamura, R. Targeted in vivo epigenome editing of H3K27me3. *Epigenetics Chromatin* **12**, 17 (2019).
28. Ichikawa, K. *et al.* Centromere evolution and CpG methylation during vertebrate speciation. *Nat. Commun.* **8**, 1833 (2017).
29. Qu, W. *et al.* Genome-wide genetic variations are highly correlated with proximal DNA methylation patterns. *Genome Res.* **22**, 1419–1425 (2012).
30. Nakamura, R. *et al.* Large hypomethylated domains serve as strong repressive machinery for key developmental genes in vertebrates. *Development* **141**, 2568–2580 (2014).
31. Takeda, H. & Shimada, A. The Art of Medaka Genetics and Genomics: What Makes

Them So Unique? *Annu. Rev. Genet.* **44**, 217–241 (2010).

32. Bhandari, R. K. Medaka as a model for studying environmentally induced epigenetic transgenerational inheritance of phenotypes. *Environ. Epigenetics* **2**, (2016).
33. Bhandari, R. K., vom Saal, F. S. & Tillitt, D. E. Transgenerational effects from early developmental exposures to bisphenol A or 17α-ethinylestradiol in medaka, Oryzias latipes. *Sci. Rep.* **5**, 9303 (2015).
34. Kungulovski, G. & Jeltsch, A. Epigenome Editing: State of the Art, Concepts, and Perspectives. *Trends in Genetics* vol. 32 101–113 (2016).
35. Steffen, P. A. & Ringrose, L. What are memories made of? How Polycomb and Trithorax proteins mediate epigenetic memory. *Nat. Rev. Mol. Cell Biol.* **15**, 340–356 (2014).
36. Barnes, P. J., Adcock, I. M. & Ito, K. Histone acetylation and deacetylation: Importance in inflammatory lung diseases. *European Respiratory Journal* vol. 25 552–563 (2005).
37. Di Croce, L. & Helin, K. Transcriptional regulation by Polycomb group proteins. *Nat. Struct. Mol. Biol.* **20**, 1147–1155 (2013).
38. Blackledge, N. P., Rose, N. R. & Klose, R. J. Targeting Polycomb systems to regulate gene expression: modifications to a complex story. *Nat. Rev. Mol. Cell Biol.* **16**, 643–649 (2015).
39. Cooper, S. *et al.* Targeting Polycomb to Pericentric Heterochromatin in Embryonic Stem Cells Reveals a Role for H2AK119u1 in PRC2 Recruitment. *Cell Rep.* **7**, 1456–1470 (2014).
40. Blackledge, N. P. *et al.* Variant PRC1 complex-dependent H2A ubiquitylation drives PRC2 recruitment and polycomb domain formation. *Cell* **157**, 1445–1459 (2014).
41. Riising, E. M. *et al.* Gene silencing triggers polycomb repressive complex 2 recruitment to CpG Islands genome wide. *Mol. Cell* **55**, 347–360 (2014).
42. Schuettengruber, B., Bourbon, H.-M., Di Croce, L. & Cavalli, G. Genome Regulation by Polycomb and Trithorax: 70 Years and Counting. *Cell* **171**, 34–57 (2017).
43. Schuettengruber, B., Chourrout, D., Vervoort, M., Leblanc, B. & Cavalli, G. Genome Regulation by Polycomb and Trithorax Proteins. *Cell* vol. 128 735–745 (2007).
44. Xiao, J. *et al.* Cis and trans determinants of epigenetic silencing by Polycomb repressive complex 2 in Arabidopsis. *Nat. Genet.* **49**, 1546–1552 (2017).
45. Laprell, F., Finkl, K. & Müller, J. Propagation of Polycomb-repressed chromatin requires sequence-specific recruitment to DNA. *Science (80-.).* **356**, 85–88 (2017).

46. Coleman, R. T. & Struhl, G. Causal role for inheritance of H3K27me3 in maintaining the OFF state of a Drosophila HOX gene. *Science (80-.).* **356**, eaai8236 (2017).
47. Qi, L. S. *et al.* Repurposing CRISPR as an RNA-guided platform for sequence-specific control of gene expression. *Cell* **152**, 1173–1183 (2013).
48. Hilton, I. B. *et al.* Epigenome editing by a CRISPR-Cas9-based acetyltransferase activates genes from promoters and enhancers. *Nat. Biotechnol.* **33**, 510–517 (2015).
49. Thakore, P. I. *et al.* Highly specific epigenome editing by CRISPR-Cas9 repressors for silencing of distal regulatory elements. *Nat. Methods* **12**, 1143–1149 (2015).
50. Cano-Rodriguez, D. *et al.* Writing of H3K4Me3 overcomes epigenetic silencing in a sustained but context-dependent manner. *Nat. Commun.* **7**, 12284 (2016).
51. Amabile, A. *et al.* Inheritable Silencing of Endogenous Genes by Hit-and-Run Targeted Epigenetic Editing. *Cell* **167**, 219-232.e14 (2016).
52. Liu, X. S. *et al.* Editing DNA Methylation in the Mammalian Genome. *Cell* **167**, 233-247.e17 (2016).
53. Morita, S. *et al.* Targeted DNA demethylation in vivo using dCas9–peptide repeat and scFv–TET1 catalytic domain fusions. *Nat. Biotechnol.* **34**, 1060–1065 (2016).
54. Lin, S., Ewen-Campen, B., Ni, X., Housden, B. E. & Perrimon, N. In Vivo Transcriptional Activation Using CRISPR/Cas9 in Drosophila. *Genetics* **201**, 433–442 (2015).
55. Jullien, J. *et al.* Gene Resistance to Transcriptional Reprogramming following Nuclear Transfer Is Directly Mediated by Multiple Chromatin-Repressive Pathways. *Mol. Cell* **65**, 873-884.e8 (2017).
56. Yamazaki, T. *et al.* Targeted DNA methylation in pericentromeres with genome editing-based artificial DNA methyltransferase. *PLoS One* **12**, e0177764 (2017).
57. Maeder, M. L. *et al.* CRISPR RNA–guided activation of endogenous human genes. *Nat. Methods* **10**, 977–979 (2013).
58. Perez-Pinera, P. *et al.* RNA-guided gene activation by CRISPR-Cas9–based transcription factors. *Nat. Methods* **10**, 973–976 (2013).
59. Lindeman, L. C. *et al.* Prepatterning of Developmental Gene Expression by Modified Histones before Zygotic Genome Activation. *Dev. Cell* **21**, 993–1004 (2011).
60. Aizawa, K., Shimada, A., Naruse, K., Mitani, H. & Shima, A. The medaka midblastula transition as revealed by the expression of the paternal genome. *Gene Expr. Patterns* **3**, 43–47 (2003).
61. Delvecchio, M., Gaucher, J., Aguilar-Gurrieri, C., Ortega, E. & Panne, D. Structure of

the p300 catalytic core and implications for chromatin targeting and HAT regulation. *Nat. Struct. Mol. Biol.* **20**, 1040–1046 (2013).

62. Tropberger, P. *et al.* Regulation of Transcription through Acetylation of H3K122 on the Lateral Surface of the Histone Octamer. *Cell* **152**, 859–872 (2013).
63. Nakamura, R., Uno, A., Kumagai, M., Morishita, S. & Takeda, H. Hypomethylated domain-enriched DNA motifs prepattern the accessible nucleosome organization in teleosts. *Epigenetics Chromatin* **10**, 44 (2017).
64. Wu, X. *et al.* Genome-wide binding of the CRISPR endonuclease Cas9 in mammalian cells. *Nat Biotechnol* **32**, 670–676 (2014).
65. Singh, R., Kuscu, C., Quinlan, A., Qi, Y. & Adli, M. Cas9-chromatin binding information enables more accurate CRISPR off-target prediction. *Nucleic Acids Res.* **43**, e118–e118 (2015).
66. Brinkman, A. B. *et al.* Sequential ChIP-bisulfite sequencing enables direct genome-scale investigation of chromatin and DNA methylation cross-talk. *Genome Res.* **22**, 1128–1138 (2012).
67. Wu, H. *et al.* Dnmt3a-Dependent Nonpromoter DNA Methylation Facilitates Transcription of Neurogenic Genes. *Science (80-.).* **329**, 444–448 (2010).
68. Tie, F. *et al.* CBP-mediated acetylation of histone H3 lysine 27 antagonizes Drosophila Polycomb silencing. *Development* **136**, 3131–3141 (2009).
69. O'Geen, H. *et al.* dCas9-based epigenome editing suggests acquisition of histone methylation is not sufficient for target gene repression. *Nucleic Acids Res.* **45**, 9901–9916 (2017).
70. Souroullas, G. P. *et al.* An oncogenic Ezh2 mutation induces tumors through global redistribution of histone 3 lysine 27 trimethylation. *Nat. Med.* **22**, 632–640 (2016).
71. Ezponda, T. & Licht, J. D. Molecular pathways: Deregulation of histone H3 lysine 27 methylation in cancer - Different paths, same destination. *Clin. Cancer Res.* **20**, 5001–5008 (2014).
72. Iwamatsu, T. Stages of normal development in the medaka Oryzias latipes. *Mech. Dev.* **121**, 605–618 (2004).
73. Notredame, C., Higgins, D. G. & Heringa, J. T-coffee: a novel method for fast and accurate multiple sequence alignment 1 1Edited by J. Thornton. *J. Mol. Biol.* **302**, 205–217 (2000).
74. Stothard, P. The Sequence Manipulation Suite: JavaScript Programs for Analyzing and Formatting Protein and DNA Sequences. *Biotechniques* **28**, 1102–1104 (2000).

75. Stemmer, M., Thumberger, T., Del Sol Keyer, M., Wittbrodt, J. & Mateo, J. L. CCTop: An intuitive, flexible and reliable CRISPR/Cas9 target prediction tool. *PLoS One* **10**, e0124633 (2015).
76. Hwang, W. Y. *et al.* Efficient genome editing in zebrafish using a CRISPR-Cas system. *Nat. Biotechnol.* **31**, 227–229 (2013).
77. Bolger, A. M., Lohse, M. & Usadel, B. Trimmomatic: A flexible trimmer for Illumina sequence data. *Bioinformatics* **30**, 2114–2120 (2014).
78. Li, H. & Durbin, R. Fast and accurate long-read alignment with Burrows-Wheeler transform. *Bioinformatics* **26**, 589–595 (2010).
79. Zhang, Y. *et al.* Model-based Analysis of ChIP-Seq (MACS). *Genome Biol.* **9**, R137 (2008).
80. Quinlan, A. R. & Hall, I. M. BEDTools: A flexible suite of utilities for comparing genomic features. *Bioinformatics* **26**, 841–842 (2010).
81. Love, M. I., Huber, W. & Anders, S. Moderated estimation of fold change and dispersion for RNA-seq data with DESeq2. *Genome Biol.* **15**, 550 (2014).
82. Chen, Q. *et al.* Sperm tsRNAs contribute to intergenerational inheritance of an acquired metabolic disorder. *Science (80-.).* **351**, 397–400 (2016).
83. Sharma, U. *et al.* Biogenesis and function of tRNA fragments during sperm maturation and fertilization in mammals. *Science (80-.).* **351**, 391–396 (2016).
84. Wang, X., Song, X. & Bhandari, R. K. Distinct expression patterns of seven crucial microRNAs during early embryonic development in medaka (Oryzias latipes). *Gene Expr. Patterns* **37**, 119133 (2020).
85. Jiang, L. *et al.* Sperm, but not oocyte, DNA methylome is inherited by zebrafish early embryos. *Cell* **153**, 773–784 (2013).
86. Potok, M. E., Nix, D. A., Parnell, T. J. & Cairns, B. R. Reprogramming the maternal zebrafish genome after fertilization to match the paternal methylation pattern. *Cell* **153**, 759–772 (2013).
87. Macleod, D., Clark, V. H. & Bird, A. Absence of genome-wide changes in DNA methylation during development of the zebrafish. *Nat. Genet.* **23**, 139–140 (1999).
88. Veenstra, G. J. C. & Wolffe, A. P. Constitutive genomic methylation during embryonic development of Xenopus. *Biochim. Biophys. Acta - Gene Struct. Expr.* **1521**, 39–44 (2001).
89. Murphy, P. J., Wu, S. F., James, C. R., Wike, C. L. & Cairns, B. R. Placeholder Nucleosomes Underlie Germline-to-Embryo DNA Methylation Reprogramming. *Cell*

172, 993-998.e13 (2018).

90. Cheung, N. K. M. *et al.* Unlinking the methylome pattern from nucleotide sequence, revealed by large-scale in vivo genome engineering and methylome editing in medaka fish. *PLOS Genet.* **13**, e1007123 (2017).

Acknowledgements

First of all, I would like to express my deepest gratitude for my supervisor, Professor Hiroyuki Takeda, and my mentor (or trainer), Dr. Ryohei Nakamura, for providing me with the opportunity to study in a splendid environment. They allowed me to proceed my challenging Ph.D. project as I want to do and brought me irreplaceable experiences. I owe my completion of my Ph.D. course to their substantial supports, encouragement, and patients.

I would like to express my gratitude to Dr. Tetsuji Kakutani for helpful discussion about epigenetic inheritance among diverse species and giving me insightful comments. Without his help, I would not have achieved to obtain Ph.D.

I would like to acknowledge all the lab members for everyday discussions and for their continuous supports. Especially, I am grateful to lab alumni, Dr. Yasuko Isoe, Dr. Napo K. M. Cheung and Dr. Kota Abe. They taught me a lot, through daily communications, about very basic but important things which I should know to achieve Ph.D. and to be a good scientist.

In addition, I would like to thank all my friends in Department of Biological Sciences for encouraging me when I faced difficulties and for giving me constructive comments and suggestions.

I would like to offer my special thanks to Jean-Baptiste Lamarck and Paul Kammerer. Their classical but intriguing ideas and experiments motivated me and took me into this field of epigenetics and inheritance. Without their previous contributions to science, I would never know such a fascinating world.

Finally, I owe my gratitude to my family. They believed in me and encouraged me all the time. I would like to dedicate this doctoral thesis to them.